

Mechanical and Metallurgical Properties of
Two-Layered Diamalloy 4010 and 2002
HVOF Coating

Yasser Abdullah Al-Shehri

Mechanical and Metallurgical Properties of Two-Layered Diamalloy 4010 and 2002 HVOF Coating

by

Yasser Abdullah Al-Shehri

A thesis submitted in fulfillment of the requirement for the
degree of

Master of Engineering (MEng)

Supervisor:

Professor M.S.J. Hashmi (D.Sc, Ph.D, CEng., FIMechE., FIEI, MASME)
Professor B.S. Yilbas (D.Eng., Ph.D, MASME)
Dr. Joseph Stokes (PhD, BAI)

Dublin City University
School of Mechanical and Manufacturing Engineering
June 2011

Declaration

I hereby certify that this material, which I now submit for assessment on the programme of study leading to the award of Master's of Engineering (MEng) is entirely my own work, that I have exercised reasonable care to ensure that the work is original, and does not to the best of my knowledge breach any law of copyright, and has not been taken from the work of others save and to the extent that such work has been cited and acknowledged within the text of my work.

Signed: _____

ID No.: 57127352

Date: _____

Acknowledgements

First of all, thanks to our creator, “Allah” for the continuous blessing and for giving me the strength and chances in completing this thesis.

Special thanks to Professor Saleem Hashmi (Head of School) and Professor Bekir Sami Yilbas and Dr. Joseph Stokes for being great advisors. Their leadership, support, attention to detail, hard work, and scholarship have set an example I hope to match someday.

I am grateful for the support of the Mechanical Services Shops Department in the Saudi Oil Company (Saudi Aramco) represented by my mentors Dr. Hussain Al-Fadhli, Dr. Alaaeldin Mustafa and Mr. Mohammed Al-Ghamdi (Head of Department). I am also grateful for the support of Martial Testing and Metallographic units at Saudi Aramco Research Center and Mechanical Engineering Department at King Fahd University of Petroleum and Minerals for supporting this research work.

My mother, father, Ali, Reem, Sara, Lama and Layan deserve special mention for their constant support and for their role of being the driving force towards the success of my project. I would like to thank my loved wife Afnan for her kindness and patience during my Master program. Special thank to my grandmother who prayed and provided me the moral support that I needed the most throughout my study.

My friends deserve recognition for lending a helping hand when I need them. Special thank to my friend Mohammed Jubran and Mohammed Al-Romaih for real friendship.

My sincere appreciation also goes to everyone whom I may not have mentioned above who have helped directly or indirectly in the completion of my project.

Table of Contents

Declaration	I
Acknowledgments	II
Table of contents	III
List of figures	VI
List of tables	VIII
Abstract	IX
1. Introduction	1
1.1 Introduction.....	1
1.2 Thermal spraying processes.....	6
1.2.1 Flame spray process.....	6
1.2.2 Arc spraying process.....	7
1.2.3 Detonation gun process.....	7
1.2.4 Plasma spraying.....	8
1.2.5 High velocity oxy-fuel (HVOF).....	11
1.3 The comparison between thermal spray technologies.....	13
1.4 Factors affecting HVOF coating properties.....	13
1.5 HVOF coating characterization.....	15
1.6 Applications of HVOF.....	17
1.7 Present work and thesis out line.....	19
2. Literature review	23
2.1 Introduction.....	23
2.2 Mechanical and chemical properties of HVOF coatings.....	23
2.3 Thermal spray powder characterizations.....	31

2.4 HVOF spraying parameters affecting coating quality	39
2.5 Thermal spray processes comparison	46
2.6 Summary of literature review.....	57
3. Experimental equipment and procedures.....	59
3.1 Introduction.....	59
3.2 Sample preparation.....	60
3.3 Surface treatment.....	60
3.4 HVOF thermal spraying system.....	63
3.4.1 Powder materials.....	63
3.4.2 HVOF equipment.....	64
3.4.3 Experimental matrix.....	67
3.5 Mechanical test preparation.....	69
3.5.1 Three point bending test.....	69
3.5.1.1 Determining Young's modulus by three point- bending.....	71
3.5.2 Tensile test.....	73
3.5.3 Vickers indentation test.....	76
3.5.3.1 Determining Young's modulus by indentation test.....	78
3.6 Metallographic Preparation	80
3.6.1 Sectioning.....	80
3.6.2 Mounting.....	81
3.6.3 Grinding and polishing.....	83
3.6.3.1 Plane grinding.....	83
3.6.3.2 Fine grinding.....	84
3.6.3.3 Fine polishing.....	84
3.6.3.4 Final polishing.....	84
3.7 Characterization analysis.....	86
3.7.1 Optical microscope.....	86

3.7.2 SEM & EDS techniques.....	87
4. Result and discussion.....	89
4.1 Introduction.....	89
4.2 Microstructure examination.....	89
4.3 Tensile and bending response of coating.....	101
5. Conclusions and recommendations for future works.....	114
5.1 Conclusion.....	114
5.2Recommendations for future works.....	117
Author publications.....	118
References.....	119

List of Figures

Figure No.	Description	Page No.
1.1	The coating layer contents.....	3
1.2	Schematic diagram of thermally sprayed spherical particle impinged onto a flat substrate.....	4
1.3	Schematic of flame gun cross section.....	6
1.4	Schematic of arc spraying process.....	9
1.5	Schematic of detonation gun process.....	10
1.6	Schematic cross-section of a typical plasma spray gun.....	10
1.7	Key components of HVOF spray system.....	12
1.8	Industrial application of HVOF.....	18
3.1	Photograph of the two types of specimens used in the tests.....	62
3.2	Grit blasting machine.....	62
3.3	HVOF Process.....	65
3.4	The three sets of the tested samples.....	66
3.5	INSTRON 8801 mechanical testing machine.....	68
3.6	Workpiece after the three-point bending test.....	70
3.7	A schematic view of three-point bending testing.....	72
3.8	The tensile test machine.....	75
3.9	A photograph of work piece after the tensile test.....	75
3.10	Indentation test equipment.....	77

3.11	Schematic view of indentation and relevant dimensions adapted from.....	79
3.12	Cut-off machine.....	82
3.13	Mounting machine.....	82
3.14	LaboPol 5 used for grinding and polishing.....	85
3.15	Optical microscope equipment	88
3.16	Scanning electron microscopy (SEM).....	89
4.1	SEM micrographs of top view of coatings produced from Diamalloy 2002 and Diamalloy 4010 powders.....	91
4.2	Roughness of the coating surfaces.....	92
4.3 (a)	SEM micrographs of cross-sections of single layer.....	95
4.3 (b)	SEM micrographs of cross-sections of two layered coatings with two different powders.....	96
4.4	EDS line scan in the coating.....	97
4.5	Optical photographs of indentation marks across the two layered coating.....	100
4.6	Optical and SEM micrograph of HVOF coated surface.....	103
4.7	Cross-sections of the single layer HVOF coated workpiece.....	104
4.8	Cross-sections of the two-layered HVOF coated workpiece.....	105
4.9	Stress-strain curve resulted from tensile tests.....	108
4.10	SEM micrographs of coating surfaces after tensile tests.....	109
4.11	Load-displacement characteristics obtained from three-point bending tests.....	112
4.12	SEM micrographs of coating surfaces after three-point bending tests.....	113

List of Tables

Table No.	Description	Page No.
1.1	Thermal spray processes characterization.....	14
3.1	Chemical composition of the coating powders.....	63
3.2	Experiment spraying parameters.....	65
3.3	The test specimen used in the study.....	67
3.4	Data used in calculating of Young's modulus from three-point bending tests.....	72
3.5	Specification of indentation hardness tester.....	77
4.1	Data obtained after indenting tests for the coating.....	99
4.2	Elastic modulus determined from three-point bending tests.....	112

Title of Thesis: Mechanical and Metallurgical Properties of Two-Layered Diamalloy 4010 and 2002 HVOF Coating

Name of Student: Yasser A. AL-Shehri

Student number:57127352

Abstract

Diamalloy 4010, which is iron/molybdenum blend, is resistive to wear and Diamalloy 2002 is resistive to corrosion and wear. However, combination of these powders in layered structure, may offer advantages over the individual powders. In this case, mechanical properties of the resulting layered structure could be improved. Consequently, investigation into mechanical and metallurgical properties of the resulting structure is necessary. High Velocity Oxy-Fuel coating of Diamalloy 2002 [(WC12Co)50,Ni33Cr9Fe3.5Si2B2C0.5] powders and Diamalloy 4010 [Fe68Mo30Cr1.8Mn0.2] powders as well as two-layered coatings consisting of these powders was carried out. In the two-layered structure, Diamalloy 4010 was sprayed at the substrate surface while Diamalloy 2002 was sprayed on the top of Diamalloy 4010 coating. The coating microstructure and morphology were examined using optical microscope, Scanning Electron Microscope (SEM) and Energy Dispersive Spectroscopy (EDS). The indentation tests were carried out to evaluate the microhardness and surface elastic modulus of the resulting coatings. The mechanical properties of the coatings were examined through tensile and three-point bending tests. It was found that the coating produced for Diamalloy 2002 resulted in higher hardness than that corresponding to Diamalloy 4010. The failure mechanism of coating during tensile and three-point bending tests was mainly crack formation and propagation in the coating. The elastic modulus of coating produced from Diamalloy 2002 was higher than that of Diamalloy 4010 coating, which was due to the presence of 12% WC in the coating. The irregularities observed in the elastic limit of the curves indicated the formation of cracks in the coatings, which was particularly true for two layered coating. The shear stress developed at interface of the two-layered coating was responsible for the crack initiation in the coating. The deep cracks were also formed in the coatings after the tensile tests. This was attributed to the local stress centers, which increased the stress intensity under the tensile load.

Chapter 1- Introduction

1.1 Introduction

Thermal spray coatings are widely used in many gas and oil industrial applications to protect the surface from various degradation processes such as abrasion, erosion, high temperature and corrosive atmosphere. In some industrial applications the deterioration mechanisms like the corrosion and wearing out of equipment components have a major role in affecting equipment durability and reliability. Thermal spray coating is a technology that includes different coating processes that provide a functional surface to protect or enhance the performance of a substrate or component. In addition, the coating process must be effective, fast and low in cost. One of the coating methods which meet these conditions is high velocity oxy-fuel coating.

A heat source melts the coating material (in powder, wire or rod form) and then the process gases accelerate the molten material to the metallic substrate to produce the desired coating as shown in the figure 1.1. As the particles exit the gun and impact the pre-coated surface, they are flattened and form thin splats or lamellae. See figure 1.2.

Thermal spray was first discovered and used in the early nineteenth hundreds and research in this field has been progressing ever since. The idea came to a young Swiss inventor, Dr. Max Schoop, after watching his son's toy canon. While his son was playing; Schoop noticed that the hot lead shot when propelled towards any surface became stuck to it. In 1914 Dr. Max Schoop ended up with an electrical arc spray [1]. Other major thermal spray processes include the detonation gun (D-Gun) system and HVOF which were invented by Union Carbide (now Praxair Surface Technologies, Inc.) in 1950 and 1958, respectively [1].

Many different types of material could be sprayed by thermal spray processes such as single phase material (like metals, alloys, ceramics and intermetallics), composite materials (like cement, reinforced metals) [2]. Cermet thermal spray coatings, consisting of WC hard particles bound with Co binder are used extensively as wear-resistant materials for many applications requiring high wear-resistant properties. These coatings exhibit superior resistance to abrasion and erosion at high temperatures and in corrosive atmospheres. Moreover, they have the advantageous combination of hardness and toughness [3].

High velocity oxy-fuel (HVOF) spraying has been widely used to spray cermet coatings. Compared to other spraying methods, high velocity oxy-

fuel spaying is one of the best techniques for depositing cermets coating [4]. This is due to the higher particles velocities and lower temperature which results in less decomposition of WC occurs during spraying. WC-Co is sprayed in many oil and gas industrial applications for requiring abrasion, sliding, and fretting and erosion resistance.

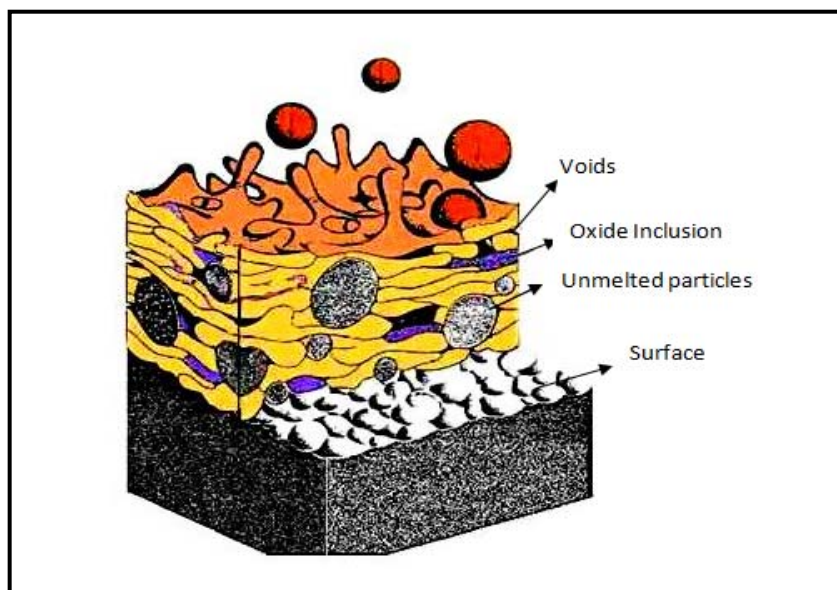


Figure 1.1 The coating layer contents [5]

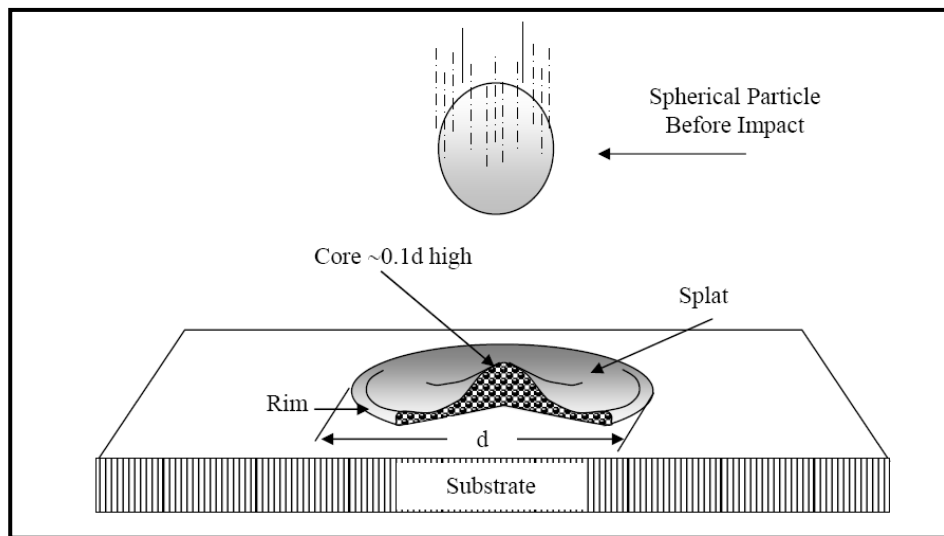


Fig 1.2 Schematic diagram of thermally sprayed spherical particle impinged onto a flat substrate [1]

1.2 Thermal Spraying Processes

The term “thermal spraying” defines a family of processes uses a heat source to melt the coating materials (in wire, rod or powder form). The molten particles are accelerated towards the substrate. Upon impact of the molten particles on the substrate surface, the particles are flattened and form thin platelets which build up the coating layers.

The family of the thermal spray processes includes flame spraying, arc spraying, plasma spraying, detonation and HVOF spraying.

1.2.1 Flame Spray Process

The flame spray process is the first spraying process developed in 1910 and still in use up to the present time. Compared with the other thermal spray processes, the flame spray process is considered the simplest and cheapest spray process. This process uses the combustion of the fuel and oxygen as a heat source to melt the feedstock material which may be in both powder or wire form (Figure 1.3). Expanding gas flow and air jets accelerate the molten coating material toward the substrate surface. Different fuel gasses may be used, using acetylene C_2H_2 as a main fuel with the oxygen ratio being the most common to produce the kinetic energy [2].

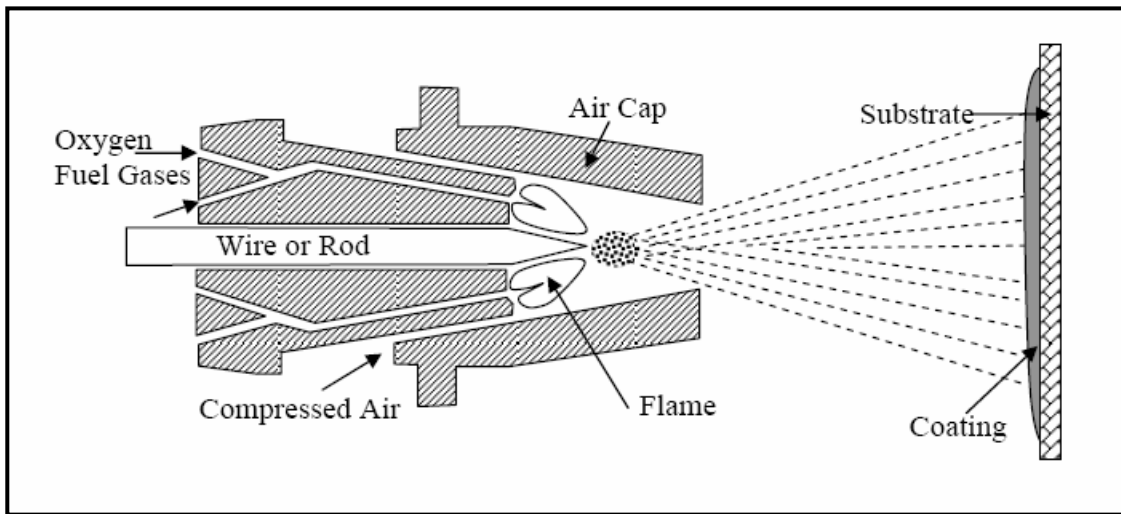


Figure 1.3 Schematic of flame gun cross section [1]

1.2.2 Arc Spraying Process

In the arc spray process, a pair of electrical conductivity wires is melted by means of an electric arc (Figure 1.4). The wire tips melt at the interesting point due to the potential differences between the wires. The compressed air atomizes and projects the molten spray material into fine droplets and projects them towards the substrate, where the molten particles impact, deform, and solidify to build up the coating [6]. Arc spraying is the highest productivity thermal spraying process since the wires are melted directly by a DC electric arc unlike the other thermal processes which indirectly heat the particles using heated gas jets.

The disadvantages of the electric arc spray process are that only electrically conductive wires could be sprayed and if substrate preheating is required, a separate heating source is needed.

1.2.3 Detonation Gun process

A detonation gun consists of a water cooled barrel with some associated valves for gases and powder (Figure 1.5). A mixture of oxygen and fuel, usually oxygen and acetylene, is fed into the barrel with a charge of powder. The system uses a spark to ignite the mixture, resulting in detonation waves which heat and accelerate the coating material

throughout the barrel to the substrate. A pulse of nitrogen is used to purge the barrel after each detonation. [2]

The velocity of the projected particles approaches 4-5 times the speed of sound [7].

1.2.4 Plasma Spraying

The plasma spray process is basically the spraying of heat softened material towards a substrate to build up the desired coating where a gas or a gas mixture is ionized by the transferred energy (Figure 1.6). This energy is released between a Tungsten alloy cathode and a copper anode [6]. The high temperature plasma flame melts and accelerates the injected coating material which is usually in powder form.

Since this process, referred to as Air Plasma Spray (APS), is commonly used in normal atmospheric conditions some oxides will always be present. Some plasma spraying is conducted in protective environments using vacuum chambers normally back filled with a protective gas such as Vacuum plasma spray in order to reduce the level of oxidation [8].

Plasma spraying has the advantage that it could spray very high melting point materials as refractory metals like tungsten and ceramics like zirconia unlike combustion processes. Due to the high temperature and velocity of the melting material in the plasma spraying process, much

denser, cleaner, and stronger coating layer is produced than with other thermal spray processes with the exception of the HVOF and detonation processes [2]. The relatively high cost and complexity of the process is considered the greatest disadvantage of the process.

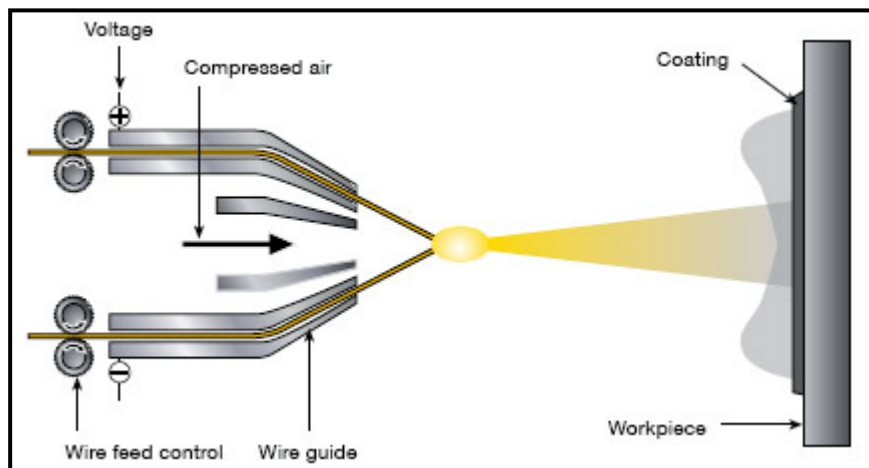


Figure 1.4 Schematic of arc spraying process [5]

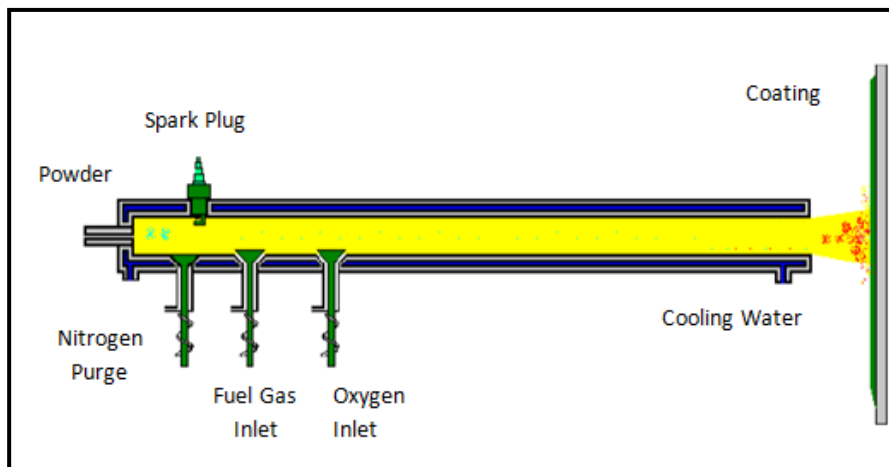


Figure 1.5 Schematic of detonation gun process [9]

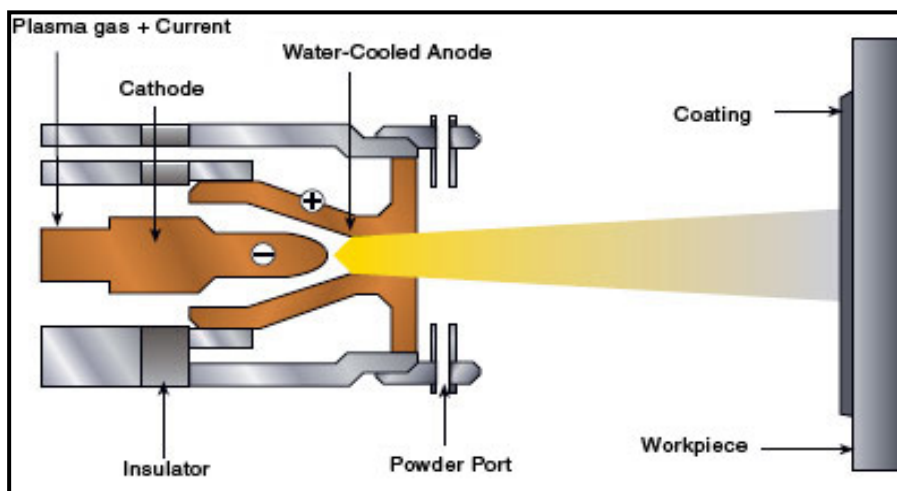


Figure 1.6 Schematic cross-section of a typical plasma spray gun [5]

1.2.5 High Velocity Oxy-Fuel

The high velocity oxy-fuel (HVOF) spraying system is a relatively new method of thermal spray techniques which could provide a very dense, tightly adherent coating with decreasing oxidation and porosity [10]. Fig 1.3 illustrates the key components of HVOF spray system. In HVOF system, a mixture of fuels such as propylene, propane or hydrogen and oxygen is injected into a gun and combusted. Powder is fed into the combustion zone using carrier gas where it becomes molten or semi-molten and then is propelled at high pressure to the substrate. The selections of the oxygen fuel and air parameters are particular to produce the desired combustion reaction.

The low porosity level and high bond strength in the coating formed using HVOF process is due to the high kinetic energy of the projected powder. There are many parameters that control the coating characterization. These parameters could be either surface preparation parameters such as grit type, blasting condition, grit feed rate a sample surface roughness or operational parameters such as flame temperature, gas pressure, powder flow rate, geometry of the nozzle and spray distance[6].

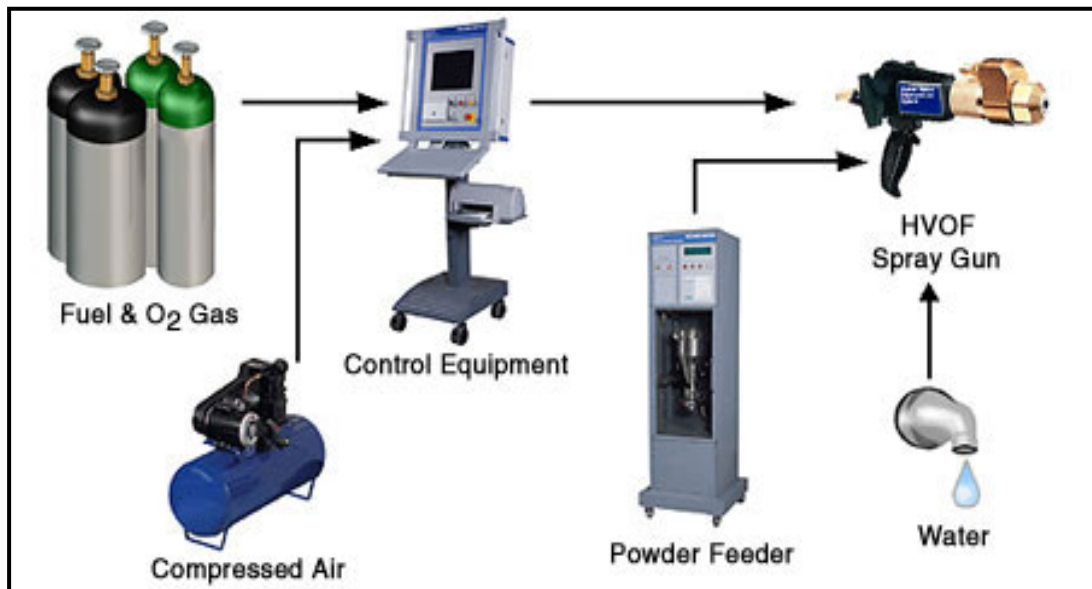


Fig 1.7 Key components of HVOF spray system [5]

1.3 The Comparison between Thermal Spray Technologies

Each thermal spray process uses two powerful characteristics of energy—heat and mechanical force in differing ways. In order to achieve a predictable and repeatable result, the appropriate thermal spray process should be selected. The selection of the thermal spray process is basically determined by the selected coating material, coating performance requirements, cost, part size and portability. The following table 1.1 summarizes the comparison between popular thermal spray technologies and how they uniquely achieve their coating characteristics [2].

1.4 Factors Affecting HVOF Coating Properties

The properties of the built up coatings layers are affected by many factors which could be classified into three categories: spraying process parameters, surface treatment of the substrate and powder properties [6]. Controlling the process spraying conditions (such as Flame temperature, feed stock delivery and gun standoff) is a main key to achieving a high protection coating layer in terms of high density, low porosity and uniform microstructure [11]. Both mechanical and chemical surface treatments are also considered as ways to obtain desired conditions or properties on the coating layer. Moreover, an appropriate selection of the powder with respect to the chemical composition, particle size

distribution, morphology and method of manufacture and apparent density plays a key role in the characterization of the resulting coating. For example, HVOF coatings which are produced by nanostructure powders show better wear and corrosion resistance the other conventional powders [12].

Table 1.1 Thermal spray processes characterizations [2]

Thermal Spray Technology	Jet Temp. (K)	Gas Flow (m³/h)	Density Range (%)	Particle Velocity (m/s)	Adhesion (MPa)
Flame spray	3500	11	85-90	50-100	7-18
High velocity Oxy-Fuel (HVOF) Process	5500	17-28	>95	200-1000	>68
Detonation Gun Process	5500	11	>95	910	82
Wire Arc Process	>25,000	71	80-95	50-100	10-40
Air Plasma Process	15,000	4.2	90-95	200-800	> 68
Vacuum Plasma	12,000	8.4	90-99	200-600	> 68

1.5 HVOF Coating Characterization

Coatings produced using HVOF characterizations have outstanding characteristics, even above other thermal spray processes. High density coating may be achieved with less than 2% porosity and some coating as low as 0.5% porosity [1].

- High bond strength. For example, typical carbide coatings sprayed with HVOF exhibit bond strengths in excess of 77 MPa. The high bond strength of HVOF coating is well affected by the effective mass of solid phase in the spray particles where the high density of solid particles led high bond strength. [13]

Other coating materials sprayed with HVOF have significantly higher bond strengths than the same materials applied using other atmospheric thermal spray processes such as air plasma spray [14].

- Improved toughness. Depending on chemistry and other factors, the short dwell time and lower temperatures of HVOF could produce wear resistant coatings with excellent impact resistance.

- Higher coating thickness. HVOF coatings exhibit high coating thickness limits where these high thickness limits are attributed to a stress relieving 'shot-peening' effect produced by the high velocity particles impacting upon the previous layers of coating. Some HVOF coatings could have a thickness up to 5.5 mm [15].

- Beneficial residual stress. Compressive residual stresses and, in some cases, very low tensile stresses enhance the fatigue life of a coated component, reduce the susceptibility of cracking and permit greater coating thickness limits.

- Wear resistance. HVOF coatings could exhibit superior resistance to sliding / adhesive wear, fretting or erosion depending on the appropriate material selection and process variables selections. [16]

- Superb corrosion resistance. The high density and exceptional metallurgical properties of HVOF coatings provide enhanced resistance to the effects of corrosion, including hot corrosion, oxidation and the effects of corrosive media such as acidic and alkaline atmospheres and liquids.

- Fine surface finishes. Smooth surface finishes allow HVOF-produced coatings to be used in the as the sprayed condition for many applications. Coatings could be machined, ground, lapped, honed or super finished to produce very high surface finishes to precise tolerances.

1.6 Applications of HVOF

Applications of HVOF and materials have a broad range across all industrial sectors (figure 1.8). Thermal spray processes are easy to use, cost little to operate, and have coating attributes that are beneficial to applications in various industries. Common HVOF surface applications are widely used in

- Aerospace field: Turbine engine fan blade mid-spans, compressor blades, bearing journals and sleeves.
- Power generation: Industrial gas turbines components such as, nozzles and blades as well as transition pieces.
- Petrochemical pump components; such as gate valves, ball valves, valve seats, exhaust stacks, sucker rods, hydraulic rods, and conveyor screws.
- Automotive: Transmission shifter forks
- General Industry: Pump housings, impellers and shafts, plastic extruders, cam followers, wear rings, machine bedways, press fits and restoration of machinery components.



Figure 1.8 Industrial Application of HVOF [17]

1.7 Present Work and Thesis Outline

High velocity oxy-fuel coating (HVOF) finds wide application in industry due to its ease of operation, low cost, and efficient processing. HVOF coatings can protect the underlying surface from the harsh environments such as high temperature, corrosion and abrasion. Depending on the coating powder properties, the resulting coating can be resistive to erosion, corrosion and wear.

HVOF process is involved in thermal spraying of powder onto the surface through which the coating is resulted. The mechanical anchoring was the only process to bond the coating to the base materials; consequently, a care is taken to improve the bonding strength between the coating and the base material during HVOF process. The selection of powders in HVOF process is based on the practical applications. In repair applications Diamalloy 4010 is used to fill the cavities in AISI 4140 steel surface. Diamalloy 4010 has almost similar elemental content of AISI 4140 steel. The cavities are formed due to high rate of erosion, corrosion and/or wear such as the cases are observed in pumps and rotating equipment casing, i.e. pump shaft wear, bearing housing and wear ring. Welding is one of the techniques used to fill the cavities. However, due to high temperature gradients developed in the welding section and high

solidification rates of the molten metal in the weld case, welding technique is not preferable in practical application. Moreover, use of HVOF coating provides many advantages over the welding technique for filling process associated with the repair applications. After filling the cavities at the surface of the alloy steel substrate, a second coating is applied for wear and corrosion protection. The coating is produced mainly from 2002 powders since it contained carbides. Therefore, in this study, single layer coating of Diamalloy 4010 and Diamalloy 2002 as well as two layers coatings of Diamalloy 4010 and 2002 are considered.

However, mechanical properties of coating produced from these powders needed to be investigated in details. In addition, coating consists of combination of the layers produced by these powders are of interest for the practical applications including gas turbine industry. Consequently, investigation into tensile and bending properties of the coating produced from these powders become essential.

In the present study HVOF spraying of powders composing of iron/molybdenum blend as well as tungsten carbide cobalt/ nickel alloy blend onto alloy steel sheets was carried out. The mechanical and metallurgical properties of the single and two layered coatings were examined. The two layered coating consists of layers of

Iron/molybdenum alloy blend and tungsten carbide cobalt/nickel alloy blend. Indentation tests were carried out to measure the elastic modulus of the coatings. Single and two layers of coating consisting of Diamalloy 4010 first layer and Diamalloy 2002 second layer were realized. The mechanical properties of resulting coating were examined through tensile and three-point bending tests.

The remaining of the thesis is divided into four chapters. Chapter Two gives a summary of relevant literature concerning HVOF spraying processing and design, equipment and theory, and applications. The literature also presents previous research on coating bending, fatigue, erosion corrosion, and tensile tests. The literature survey is classified according to four categories which were (i) mechanical and chemical properties of HVOF coatings (ii) thermal spray powder characterizations (iii) HVOF spraying parameters affecting coating quality and (iv) thermal spray processes comparison.

The trial equipment and procedures are described in chapter three. This chapter is divided into seven main sections, which includes introduction, full descriptions of sample preparation, surface treatment, HVOF spray system used, mechanical experimental tests, metallographic preparation and characterization analysis. The mechanical tests sample preparation,

which is the core of this work, consists of three parts which are three point bending test, tensile test and Vicker's indentation hardness test.

Chapter four presents the experimental results and discussion. The mechanical test results are shown separately in two parts. The mechanical tests were conducted to understand the characterization of the coating multi layers interface and coating base interface.

Finally, the overall conclusions drawn from the results are summarized in chapter five. The recommendations for future work in this area are provided after the conclusions.

Chapter 2- Literature Review

2.1 Introduction

The following section is a brief review of the earlier studies carried out in this field with special attention to HVOF coating parametric, microstructural and mechanical properties. The literature review of this thesis is characterized under four topics which are (i) mechanical and chemical properties of HVOF coatings (ii) thermal spray powder characterizations (iii) HVOF spraying parameters affecting coating quality and (iv) comparison between thermal spray processes.

2.2 Mechanical and Chemical Properties of HVOF Coatings

Stewart et al. studied the influence of the different heat treatment process on the abrasive wear resistance of HVOF thermally sprayed WC-Co coating [18]. The range of the heat treatment was between 250 °C and 1100 °C. The results showed that coating started the changing formation of $\text{Co}_6\text{W}_6\text{C}$ from the amorphous phase when the heat treatment was above 600 °C. It was found that the heat treatment always reduced the residual

stresses of the coating due to the thermal expansion mismatch between the coating and the substrate. In addition, cracks were produced in the coating layer as a result of the reduction of the residual stress. An improvement in the abrasive wear resistances was observed because of the micro cracking and the lower residual stress level on the coating. It was noticed that the low heat treatment temperature was an adequate method to enhance the abrasive wear behavior of the coating since the high temperature caused large scale cracking of the built coating.

Padilla et al. conducted an experiment in order to study the effect of Ni-5 Mo-5.5 Al (wt. %) applied by HVOF, on the fatigue properties of AISI 4140 steel [19]. The investigation was carried out by comparing the fatigue behavior of uncoated samples with those of the specimens after grit blasting and after blasting and coating with such a deposit. Tensile tests and fatigue test were carried out. Grit blasting could be used to induce compressive residual stresses into surfaces. The experiment found that grit blasting gave rise to a significant decrease in the fatigue properties of the material. Further coating of the grit blasted samples, applied by HVOF, led to a further reduction in the fatigue strength of the material. It had been suggested that such a further decrease was mainly associated with two different causes. First, the extensive fracture and delamination of the coating from the substrate had been observed from

the microscopic analysis. Secondly, the possible existence of tensile residual stresses in the substrate, in the vicinity of the substrate deposit interface which would assist in the propagation of the fatigue cracks nucleated at the alumina particles.

Guilemany et al. studied the influence of the coating thickness deposited by HVOF with multi layers of $\text{Cr}_3\text{C}_2\text{-NiCr}$ in the corrosion properties. Steel was used as a substrate material [20]. Various numbers of electrochemical measurements were carried out such as Open-Circuit Potential (E_{oc}) and polarization Resistance (R_p) in NaCl media. The corrosion process was analyzed by performing Electrochemical Impedance measurement. Further microstructure tests were carried out. It was found that the level of porosity and cracks in coatings resulted in different values of resistance and capacitance. Moreover, it was noticed that the cracks between obtained layers and the stress generated on the coating layer played a main role for the electrolyte to pass through thicker coating. It was also observed when thin coating layer produced; a low anticorrosive behavior was resulted because the coating layer was not adequate to close the system against the pass of electrolyte. Therefore, controlling the stress generation during the spraying was required when cermet coating applied on base steel.

A comparison experiment was carried by Stoica et al. to investigate the sliding wear behavior of as sprayed and Hot Isostatically Pressed (HIPed) thermal spray cermet coating deposited by HVOF [21]. WC-12C coating powder was sprayed by HVOF on bearing steel substrate followed by HIPed at 850°C. For each specimens, a sliding wear test was conducted using steel and ceramic reciprocating balls on-plate at a sliding speed of 0.03 m/s and load 4-6 N. The coating was characterized using X-Ray Diffraction (XRD), Scanning Electron Microscope (SEM) and Micro-hardness test. Results of the study revealed that a sufficient enhancement of thermal spray cermet coating wear resistance was observed by hot isostatic pressing post treatment where this offered about 100% improvement in wear behavior of cermet coatings. This enhancement in physical characterizations was due to the phase transformations where secondary phase W_2C and metallic tungsten were eliminated, alteration of amorphous binder phase through recrystallization of Co leading to precipitation of the η carbides. After HIPing post treatment the coatings modulus found to be increased as a result of the metallurgical bonding improvement. Depending on the results of tribological testing, it was noticed that the wear mechanism had a main effect on the amount of lost material.

Fedrizze et al. evaluated the wear corrosion behavior of HVOF coating and compared it to that of hard chromium plating [12]. Both conventional and nano size of Cr_3C_2 based cermet powder were deposited by HVOF process. Steel samples with disk geometry were machined and used as substrate. A special apparatus was designed to conduct both of electrochemical and mechanical analysis. This test was carried out under three conditions (i) free corrosion no applied polarization) (ii) only lubricated wear by applying cathodic polarization (iii) forced corrosion by applying an anodic current. It was found that HVOF degradation mechanism was lower than that of conventional plating because of the presence of ceramic components in the former. The results indicated that HVOF nano powder coatings showed better resistance among the other conventional due to the low porosity, low surface roughness and better distribution of chromium carbide in the metal matrix.

The wear behavior of the optimized WC-VC-Co coating deposited by high pressure high velocity oxy-fuel was compared to the commercial WC-Co coating by Machio et al.; taking into account a similar experimental work was conducted with non-optimal WC-VC-Co powder, where no enhancement in VC containing powder was observed with a comparison with that one of Commercial WC-Co [22]. The abrasion test was performed in both dry and wet condition as well as slurry erosion

test. The results revealed that WC-VC-Co coating showed higher abrasion behavior in both test conditions than that one of commercial WC-Co. This was due to the presence of VC phase which played a role in obstructing the growth of WC grains, enhancing the corrosion behavior of the coatings and forming the (V,W) C, which reduced the volume fraction of cobalt since it had lower density than the WC phase. However, no sufficient improvement of the optimized coating slurry erosion resistance was noticed where it almost behaved in the similar way of the commercial powder.

Wielage et al. carried out three studies in order to develop the high velocity oxy-fuel spraying system [23]. Firstly a study was conducted to evaluate the wear behavior of cermet coating deposited on light weight material parts subjected to dynamical load. The second study, using advanced HVOF gun with high combustion chamber pressure to reduce the particle temperature was investigated. From financial point of view, ultrafine powder instead of conventional size powder was considered as third case. This was because that the cheap belt grinding could be used to finish the former coating. It was found that HVOF cermet coatings applied on light weight material showed an excellent wear behavior without detracting of fatigue strength. Depending on the results, nickel or iron base coating deposited by high combustion pressure had high

corrosion resistance due to high density and low oxygen content in the coating. More consideration must be attended in case of replacing the conventional size powder with ultrafine powder. Even though ultrafine powder behaved better than the conventional one, a low dry abrasive wear resistance was noticed for the ultrafine powder coatings. Therefore, short life time of components may be resulted, because of the reduction in the cermet coating costs.

Al-Fadhli et al. carried out an experimental to study the erosion corrosion resistance of plain and welded stainless steel substrates compared to a compound material of stainless steel and carbon steel all coated with Inconel-625 alloy obtained by HVOF thermal spray process [24]. Two fluids conditions were used to evaluate the erosion-corrosion properties of three samples categories. These conditions were (i) free from add solids and (ii) containing 1% silica sand. A jet impingent rig was employed to perform the test. SEM and EDS were used to investigate the microstructure of coating. The results indicated that the locations of non-molten and semi-molten particles were the source for the removed material. Moreover, the types of substrates material did not show any influence of the erosion-corrosion behavior. A catastrophic failure in the coating was observed when the impinging fluid hit the sample surface, especially, in case of carbon steel substrates. According to the experiment

results, an increment of 50% in the removal material rate was recorded, in case of using fluid with 1% silica sand, with comparison to use free fluid from added solids. It was found that the removal material rate increased as the flow of slurry fluid increased. The type of the substrate was also played a main role in this increment.

The scratch resistance and corrosion properties of the nanostructured WC particle-polymer coatings were investigated by Wang et al. [25]. The samples were prepared in various conditions, pure polymer coating, polymer coating + 10% solid particles and polymer coating + 20% solid particles. Carbon steel was used as a substrate. Hardness, scratch and corrosion tests were carried out. According to the experiment results, a sufficient enhancement in the nanostructured WC particle/polymer coating was observed with comparison with that one of the pure polymer coating. This could be due to the particle strengthening of nanostructured WC particle. In addition, the corrosion test revealed that the corrosion properties of the nanostructured WC particles/ polymer composite coatings found to be higher or at least equivalent to that of the pure polymer coating.

Summary

The mechanical and chemical properties of HVOF coating were investigated by many researches [18-25]. The main concerns were the change of the compounds in the coating due to oxide formation during the spraying process and the carbide particles distribution in the coating. In addition, the influence of heat treatment on the coating mechanical and chemical properties was also considered. However, the findings were subjected to spraying parameters and powder properties, namely percentage of carbide content and the powder type. Therefore, the generalized conclusion for the optimum spraying parameters for all powders was left obscured. In general, the findings revealed that increasing oxygen content enhanced the brittleness of the coating while reducing the fracture toughness. Inclusion of carbide in the powder enhanced the surface hardness. However, homogeneous distribution of carbide in the coating had not been reported.

2.3 Coating Powder Characterizations

Tan et al. studied the repair of worn components using HVOF thermal spray [15]. Stainless steel was used as coating material as well as substrate to restore the worn parts to their original dimensions. In addition, two more types of specimens were prepared which were 2D tool steel and nitride tool steel substrates. Both tool steel matching powder

(Diamalloy 4010) and tungsten carbide cobalt were used as repair material for the tool steel substrates. Grooves were machined on the specimen with various depth dimensions. The samples were tested under three conditions (i) stainless steel powder on stainless steel substrate (ii) tool steel match powder on tool steel substrates (iii) tool steel match powder on nitride tool steel substrate. It was found that HVOF thermal spraying process could be extremely useful as an excellent technique to repair and restore damages with various depths in 2D tool steel substrates. The thickness of 5.5 mm could be achieved if the properties of the coating material with the substrate material were matched. It was also showed that WC-Co wasn't an appropriate selection to be used in such repairs. Depending on the microscopic analysis, a strong bond was observed between the coating layer and the substrate for all the adequate repair samples. However, the repair material faced a difficulty depositing (or: forming a deposit) on the nitride tool steel substrate due to the hardness of the nitride surface. Therefore, more time was necessary to repair the nitride surfaces.

Unreinforced and reinforced molybdenum disilicade coatings deposited by HVOF thermally spraying was investigated by Reisal et al. in term of oxidation [26]. The test specimens were prepared as low porosity unreinforced MoSi₂, high porosity unreinforced MoSi₂, reinforced MoSi₂

with silicon carbide and reinforced MoSi₂ with alumina. The samples were subjected to high temperature 5000°C, 1000 °C and 1500 °C. Scanning Electron Microscopy (SEM), Energy Dispersive X-Ray analysis (EDX) and X-Ray Diffraction analysis (XRD) were used to evaluate the coating characterization. In addition, the simultaneous thermo gravimetric equipment was employed to study the oxidation behavior. It was noticed that the porosity of the coating had a gradual effect on the peening reaction of the MoSi₂ at 500 °C. An increase of the peening reaction was noticed in case of silicon carbide as reinforced phase, whereas alumina reduced that peening reaction. At 1000 °C, the tests showed that no effect was observed of the heating rate on the short term oxidation properties. Moreover, no defect was addressed on all tested samples after 60 hours oxidation. At 1500 °C, a protective SiO₂ layer was formed with a thickness of 10 µm for the unreinforced MoSi₂ coating.

Totemeier et al. studied the characterization of microstructure and stress in Fe₃Al coating generated by HVOF thermal spraying [27]. The nature of the peening stress was tested by studying coatings which had been prepared at three different torch pressures, corresponding to three different particles velocity. Residual stresses in the coatings were characterized by curvature measurement and X-Ray Diffraction (XRD). Line broadening analysis and coating micro hardness

measurements were performed to characterize the extent of cold work in the coating and its effect on strength. XRD was also used to indicate thermal expansion coefficients of the coating in-situ on the substrate. It was found that HVOF practical velocity strongly affected the microstructure, residual stress and hardness in HVOF thermally sprayed Fe₃Al Coating. Higher Velocity gave rise to increasing compressive residual stresses due to increased peening effect. Residual stresses vary from nearly zero for coating prepared at 390 m/s to approximately 450 MPa for coatings prepared at 630 m/s. Good agreement was found between residual stresses measured using XRD and those calculated from coupon curvature. X-ray line broadening analyses revealed a corresponding increase in the extent of cold work present in increasing microhardness with particle velocity. Yield stresses calculated from the microhardness values were high for Fe₃Al Alloys, ranging from 610-1180 MPA. The microstructures of coating prepared at higher velocities show more signs of deformation and fewer unmelted particles. The coefficient values obtained using x-ray analysis of as sprayed coatings were significantly lower than those for powder and bulk alloy, primarily due to the presence of residual stresses at low temperature. The mean CTE values for annealed coating more closely matched the powder data, but were still slightly lower.

Trompeter et al. studied the oxides the particle characterizations of NiCr powder deposited by high velocity air fuel in term of structure and composition and the behavior of particle during the spraying was also considered [28]. Aluminum, Cu and Fe were used as substrates to spray NiCr coating with different layer thickness ranging from individual splats layered to a layer of 1 mm thickness. The composition of the powder was 95% NiCr with a small amount of Si and 5% of Si/Cr. Scanning Electron Microscope (SEM), Nuclear Reaction Analysis (NRA) and X-ray Photoelectron Spectroscopy (XPS) were employed to characterize the coating material where the later two methods used to examine the surface oxides. The experiment results indicated that during the spraying no extra oxides formation at the surface and coating bulk took place. Moreover, no change on the powder particle composition was observed. In addition an oxides mixture of Ni, Cr and Si with thickness of 7 nm was noticed at the surface. Since Si considered as a deoxidizer besides it customized the viscosity of the molten metal during, it was added to enhance coating properties.

Pure molybdenum and molybdenum blends coatings deposited by atmospheric plasma spray were investigated by Hwang et al. in order to study the influence of coating microstructure on the wear behavior [29]. Five types of powder were prepared (i) as pure Mo, (ii) Mo blended with

brass, (iii) Mo blended with bronze (vi) Mo blended with Al-Si (vii) Mo blended with bronze and Al-Si. Carbon steel was used as a substrate. Microstructure, hardness and wear analysis were carried out. It was found that coating deposited with pure Mo had higher hardness and lower wear rate than the other four Mo powder in both coating and counterpart material, whereas the friction coefficient decreased. In addition, higher hardness and higher wear behavior were observed for the coating obtained of Mo mixed with bronze and Al-Si with comparison to other Mo blended coatings. In this case, a reduction in the counterpart wear rate was noticed.

Investigation into bond strength of Ni and Co composite powders blended with carbides and sprayed by HVOF process onto mild steel surfaces was carried out by Wang et al [13]. Various types of Ni (Co) based composite powders consisted of material of high melting point including WC, SiC, TiC, Al₂O₃ and W, beside two other large Ni- based metallic powder. Spray the particle in a solid liquid two phase condition was created by the design of the powders. It was found that the bond strength of HVOF coating was correlated well with the spraying parameters, except temperature and particle velocity. The bond strength of coatings was varied from 20 MPa to over 77 MPa. The result indicated that the bond strength of HVOF did not show a direct correlation with the conventional

state conditions of the spray particle, i.e. temperature, velocity and momentum. By contrast, a correlation between high bond strength of HVOF coating and effective mass of solid phase in a spray particle proposed was noticed. According to the experiment result, in order to ensure high strength of HVOF coating besides the solid liquid two phase condition, a high density of non-melting phases in a solid liquid two phases was required.

Hu et al. studied the properties of NiAl nanostructured coating produced by HVOF spraying [30]. Ni and Al compound powder in the atomic ratio 50:50 were milled under Ar gas atmosphere. X ray- diffraction and scanning electron microscopy (SEM) coupled with energy dispersive spectrometry analysis (EDS) were used to examine the coating properties. It was shown that increasing the milling time reduced the grain size of the powder and increased the lattice constant. It was also found that HVOF thermal spraying of milled metallic powder was effective for producing Ni Al nanostructure coatings. Based on the experiment measurements, the grain size, lattice constant, hardness and elastic modulus of the studied coatings were 10.4 nm, 0.290 nm, 7.61 GPa and 180 GPa. It was observed that microhardness, dynamic hardness and elastic modulus of the as deposited coating decreased as heat treatment increased. In

addition, increasing temperature led to a decrease in the high temperature hardness.

The deposition behavior of single WC-Co spray particle impacting on the substrate with various hardness using cold spraying process was studied by Gao et al. Three nano sized WC-12Co powders with different porosity were used in order to change the ability of deformation on impact [31]. The porosity of three powder were changed from 44%, 30% to 5% and the microhardness were changed from 78Hv, 548Hv to 1317Hv. Stainless steel and two nickel based self fluxing alloys, which were coated on stainless steel substrate, with different hardness (200Hv, 500Hv and 800Hv) were used as substrates. It was showed that the two WC-Co powders with high porosity 30% and 40% could be deposited on stainless substrate with various level of hardness. However a soft stainless surface had to be used to deposit low porosity powder of a hardness of 1317Hv. Moreover, the deposition of the coating particles was mostly assigned to the deformation of the powder. It was found that appropriate selection of the designed porous cermet powder with a specific hardness of substrate played a mainly role to deposit hard WC-Co cermet coating by cold spraying.

Summary

The characterization of HVOF was important since it had a significant effect on the coating properties. This was particularly true for multi compound powders such as carbide. In addition, the molten states and solidification of powders in the coating was found to be affecting considerably the mechanical properties of the coating such as tensile fatigue and hardness. The studies presented in the open literature considered different powders and findings of the mechanical properties were associated with the powder characteristics. In general, carbide powder acted as stress centers in the coating initiating the cracks. The fast solidification rates of the molten powders found to affect the coating hardness.

2.4 HVOF Spraying Parameters Affecting Coating Quality

Gourlaouen carried out an experimental study on stainless steel substrates to address the influence of the spray variables on the coating characterization [32]. HVOF spraying process was widely used to improve components life in service. However many variables could effect metallic coating properties, particularly un-melted particles and oxidation level. Flame parameters such as combustion ratio, temperature, were of prime importance. The conclusion of this study showed that the influence

of the combustion temperature was small. On the contrary, an increase of the flame power led to higher the oxidation with low unmelted particles rates and the deposition efficiency was improved. Among the three parameters studied, the combustion ratio had significant influence. Its increase, in the domain considered, was involved with a decrease of the oxygen content, and consequently of the microhardness, but an increase of the number of unmelted particles resulted in a decrease of the deposition efficiency.

The effect of HVOF spray condition on molten particle velocity and surface temperature was examined by Wei et al. [33]. Carbide/nickel-chromium alloy was used as a coating material. The HVOF spray parameters evaluated were oxygen fuel rate, fuel gas flow rate, powder carrier gas flow rate, powder feed rate, gun barrel length, stand-off distance and substrate surface speed. The microstructure and mechanical properties of the coating were examined. It was also observed that the feed stock rate, standoff distance and gun barrel length played a main role in the output temperature of the molten particle. According to experimental results, a sufficient enhancement in abrasion wear resistance was observed by depositing coating at higher particle velocity. However, coating deposited by molten particles that were heated at high

temperatures, ranging from 1650 °C to 1725 °C, showed lower porosity content of the coating.

Kuroda et al. investigated the relationship between the conditions of sprayed particles in flight and stress generation during deposition [34]. 316 L stainless steel was employed for both the sprayed powder and the substrates to eliminate the stress due to difference in thermal expansivity. Powder size and the velocity of particles were varied in order to control the kinetic energy. It was found that a strong negative correlation existed between the temperature and diameter. In contrast, the correlation was very weak between the diameter and the velocity. The process of the stress generation of the HVOF coating was more complicated compared to conventional thermal spray processes because of the peening action of the particles. The depth of peening effect could be as much as 50 µm. The intensity of peening action was correlated with kinetic energy of sprayed particles. The Peening stress in the steady state depended on the properties of both coating and sprayed particles, and the stress value ranged from 200 MPa to an almost negligible level. The results revealed that a broad window for the stress control was available through the control of spray parameters with the HVOF process.

Totemeier et al. investigated the effects of HVOF spray parameters on spray particle characteristics, deposition efficiency, and residual stresses and studied the use of an XRD technique for residual stresses measurement in HVOF coatings [35]. Fe₃Al and AISI type 316 stainless steel coating materials were tested. Three different spray conditions were studied for each material; the spray particle characteristics (size, distributions, velocity,) were assessed for each material and spray condition. The XRD based residual stress measurement were made for each material and spray condition on a series of coatings with varied thickness sprayed onto thin deforming and thick non-deforming substrates. Moreover the factors in the X-Ray and measurement and HVOF were discussed. It was found that increasing torch chamber pressure resulted in increasing spray particles velocity with little change in the spray particles' temperature. Relative deposition efficiencies were maximized at an intermediate particle velocity. The reduction at high speed velocity was due to increased splashing of the impacting droplets. Residual stresses in coating on thin substrates became slightly less compressive with increasing coating thickness.

Totemeier et al. applied Fe₃Al coating by HVOF thermal spray technique with various spray particle velocities in order to evaluate the influence of

the former on the micro structure, residual stress, tensile properties and thermal-expansion coefficients [36]. The residual stresses were determined as a function of coating thickness using curvature measurement. Three different torch chambers pressures 340, 517, and 620 kPa were set to obtain the coating on carbon steel substrates, where the resulting particle velocity was 390, 560 and 620 m/s, respectively. In addition, the test specimens were annealed for 2 hours at 800° C. According to the experiment's results, compressive residual stress and heavily cold worked microstructure were observed in the coating. This peening effect was due to the additional high velocity impact in the underlying layers. Moreover, increasing the particle velocity led to an increase in the peening effect's magnitude. It was also found that increasing the coating thickness produced an increase in the coating-substrate miss-match strain. At room temperature, all coatings had a brittle behavior. However, a sufficient increase of the fracture stress was recorded by increasing the particle velocity, which ranged from 60 to 90 MPa at 390 m/s to 380-400 MPa at 620 m/s. In some cases, annealing treatment caused an enhancement of fracture stress because of the elimination of internal and local stress. Lower coefficient thermal expansion values for coating compared to those of wrought Fe₃Al was also observed.

Lima et al. optimized the spray parameters of the HVOF Titania coating and compared the results with an earlier research on HVOF Titania coating [11]. In order to optimize the spray parameters a diagnostic tool was used to measure the particle temperature, velocity and diameter in the spray jet. The results showed that optimizing the spray conditions led to sufficient enhancement on the coating properties such as high density, low porosity and uniform microstructure in the produced coating in comparison to the earlier research.

The effect of spray conditions on the particle in flight properties and the properties of HVOF coating of WC-CoCr was investigated by Zhao et al.[37]. The particle size distribution of WC-CoCr powder was $-45 + 11$ μm . The microstructure, hardness and wear behavior of the coatings were evaluated. The results indicated that the particle and coating characterizations reached different levels because of spray parameters such as the total gas flow rate, the powder feed rate and standoff distance. It was found that high particle velocity and high particle temperature were caused by increasing the total gas flow rate and lowering the powder feed rate with a short standoff distance. The particle velocity showed more sensitivity to spray parameters than the particle temperature. In addition, increasing the particle temperature and velocity led to enhancing the coating hardness and decreasing the porosity. According to the study

results, the total gas flow rate was observed to be a more effective parameter than powder feed rate, which had more effect than standoff distance.

Hasan et al. made an experimental study to show the influence of the spray variables on residual stress build up of HVOF spray aluminum/tool steel functionally graded coatings [38]. Many parameters could affect the residual stress generated on the obtained coating, such as flow rate ratio oxygen to propylene, compressed air flow rate and spray distance. The aim of their work was focused on the influence of those parameters on the residual stress. It was showed that among the three parameters studies, the spray distance had significant influence on the residual stress. Its increase led to increase the flight time of the particles which in turn, lower the impact velocity and temperature. In addition, the optimized set of spray parameters of Aluminum powder in order to obtained low residual stress with high thickness coating was addressed 4.5 oxygen to propylene ration, 270 Standard Liter Per Minute (SLPM) and spray distance of 225 mm. In case of depositing functionally graded material coatings, it was suggested to use the variables for the lower boiling point temperature material since using the parameters for the higher boiling point temperature may led to lose the lower boiling point material during spraying.

Summary

The spraying parameters such as spraying distance, jet pressure, flame temperature and particle velocity were found to be important effecting the resulting coating both mechanical and metallurgical properties. The findings revealed that inverse relation was existed between flame temperature and flame area. In this case, the surface hardness of the coating changed when spraying temperature changed. However, the in-flight time influence the oxidation rate of the powder sprayed. Layer the in-flight time results in more the oxidation formation around the splats while affecting the surface hardness and brittleness of the coating.

2.5 Thermal Spray Processes Comparison

The mechanical properties of MCrAlY coatings sprayed by HVOF system were analyzed by Itoh et al. in comparison with the vacuum plasma sprayed MCrAlY coatings [8]. Moreover, the characteristics induced by HVOF system were investigated using the deflection measurement X-ray method in comparison with the air plasma spraying (APS) system. It was found that in the case of HVOF, the microstructure revealed even the as-sprayed that coatings were very dense with low oxide content as normally found in plasma sprayed coating in the open air. This was because there were a lot of poorly melted particles. The heat

treatment after thermal spray transformed the coating layer into uniform microstructure with two predominant phases. A fair amount of porosity ($> 3\%$) of HVOF was reduced by applying the diffusion heat treatment. with respect to bending strength & Young's modulus of HVOF were poorer in compression with the VPS coating. However, the level of HVOF coating could be enhanced up to the level of VPS coating by applying the heat treatment. These phenomena could be due to the poorly melted particles in the coating layer of HVOF. On the other hand, there was no difference for Vickers hardness of coatings sprayed by HVOF and VPS. Moreover, the Vickers hardness of heat treated HVOF showed high value in compression with the VPS. This was caused by the HVOF process for own sake such as carbonizing some elements of MCrAlY coating from the Kerosene + Oxygen fuel. According to the rise in temperature during the process, HVOF revealed a higher temperature in comparison to the ABS system. This meant the high deposit of the HVOF system was due to the very high particle velocity. It was clear that the surface temperature and the displacement became high values with the increase of the combustion gas pressure. The deformation behavior of the cantilever beam was strongly affected by the peening due to the poorly melted particles, and not by the temperature rise that causes the concave deformation. The residual stress analyses showed that the residual stress

of HVOF was reduced by the peening effect in comparison with the plasma a spray system in air.

Shimizu et al. made an experimental study on the enhancement of HVOF coating deposition efficiency and hardness [39]. Three different guns of varied geometry were designed and tested experimentally. The spraying process was simulated numerically for each of the nozzle geometries to understand their effectiveness in influencing the velocity and temperature of the sprayed particles. The coating was characterized using Optical and Scanning Electron Microscope (SEM), Micro-Vickers hardness test and X-Ray Diffraction (XRD). Results showed that with the use of convergent and divergent gun type nozzle, the extent of the melting of the alumina particles would be increased. This was exhibited by an increase in the deposition efficiency (amount of material adhered to amount of material sprayed) to extent of 45%. However, the sharp change in the convergent and divergent nozzle geometry, results in fusion agglomeration of alumina particles leading to spitting during the spraying process. The result showed that alumina coating of excellent hardness 920-1290 HV with a relatively microstructure could be obtained in HVOF method irrespective of the gun nozzle geometry, providing the spraying parameters were properly controlled.

Nascimento et al. analyzed the effects on the AISI 4340 steel, in the rotating bending fatigue behavior, of the tungsten carbide thermal spray coating applied by the HP/HVOF process, chemical nickel underplate, and shot peening process applied before coating deposition, in comparison to hard chromium electroplatings [40]. The rotating bending test showed that the effect of HVOF and hard chromium plating was to decrease the fatigue strength for AISI 4340 steel. The decrease in the fatigue strength was higher in the chromium electroplated sample than in the tungsten carbide coated samples. This may be due to HVOF compressive residual internal stresses which were formed from mechanical deformation on surface during particle impact. The observed reduction in the fatigue strength of steel, despite the compressive residual stress included by the HVOF process may be associated to the high density of pores and oxide inclusions into coating. Analysis of the tungsten carbide coating showed that the aluminum oxide blasting was responsible for the increase in roughness at the interface substrate-coating, increasing after adhesion. The higher rotating bending fatigue strength of the conventional hard chromium in comparison to the accelerated hard chromium electroplating, may be related to the lower microcrack density of the conventional hard chromium electroplating. For both HVOF and chromium electroplating no change in microstructure

was observed. The results indicated higher fatigue strength for the lower chromium thickness. The shot peening pre-treatment proved to be an efficient process to improve the fatigue strength of hard chromium electroplated components. The hard chromium electroplating and the electroless nickel plating proved to have excellent adhesion when applied on steel.

Ahmed et al. carried out an experiment in order to understand the mechanisms of fatigue failure in thermal spray coatings in rolling and sliding contact [41]. Detonation gun (D-Gun), high velocity oxy-fuel and high velocity plasma spraying (HVPS) techniques were used to deposit cermet (WC-Co) and (Al_2O_3) coatings on steel substrates. The thickness of the coating varied from (20-250 μm). The role of spray variables, substrate material characterization and thickness on the fatigue failure was studied. Microstructure examination such as XRD and SEM were carried out. Depend on the results, four modes of fatigue failure were addressed which were abrasion, delamination, bulk failure and spalling. It was found that considering the contacting material pair and lubricant condition could limit the abrasion failure. It was also noticed that optimizing the coating thickness and toughness fracture had an impact on the delimitation failure. However, no delamination failure was observed during the test when the contact stress was lower than 2.0 GPa. For In

bulk failure mode, it was observed that considering the hardness of the substrate as well as an increase in its thickness could transform this mode of failure. It was found that spalling may originate from surface or subsurface and it was the least seen failure mode in thermal spray coating.

Wang et al. studied the effects of coating structure and spraying method on coatings properties, single layered WC-Co coatings and multi-layered coating consisting of WC-Co and NiCrAl manufactured by detonation spraying (DS) and HVOF [42]. The mechanical and anti-wear properties were tested for the four coatings to measure porosity, microhardness and the residual stress levels. The thermal shock experiment and the wear test were also performed. The gradual change of properties in multi layered structured decreased the residual stress. The HVOF single layered coating exhibited the least variation of the weight loss rate among the four kinds of coatings. The thermal shock property of HVOF multi layered coatings was found to be the best among other residual stress. With light loads the wear rate of HVOF multi layered coatings increased with sliding speed. In contrast, under heavy load, the weight loss rate decreased with sliding speed. More deep pits lifted on the worn surface with heavy load and slow sliding speed. However, with high speed the worn surface was absorbed to be smooth. The weight loss rate of the HVOF single layered

coatings increased with sliding speed and load. Consequently, mechanical properties of HVOF coating were better than those of the detonation spraying coatings. Spraying method and the coating structure affected the residual stresses. Residual stresses of detonation spraying multi layered coating were only 50% of the detonation spraying single layered, where as the coating structure had less affected on the residual stresses in HVOF coatings. Multilayered coatings had better sliding wear resistance, especially at light load compared with the single layered.

A comparison study was carried out by Sampath et al. between air plasma spraying, wire arc spraying and HVOF spraying in order to investigate the influence of the temperature and velocity on the properties of the applied Ni-5wt.%Al coatings' on steel substrates [43]. Besides thermal spray process, the cold sprayed process was included in the study. In flight particle diagnostics, porosity, elastic modulus and thermal conductivity were evaluated in the specimen coating. The stress strain relationship was also analyzed. The authors found that the elastic modulus, thermal conductivity and hardness of the cold sprayed process were lower than that of HVOF coating. This was because of the high presence of non-metallurgically bonded interfaces. This revealed that increasing the in-flight particle velocity alone resulted in a dense structure in terms of volume porosity. It was also found that the HVOF coating had

better mechanical characteristics among the other processes. This was true for the plasma and wire arc spray processes due to the high porosity of the coating. The lack of metallurgical bonding in the cold sprayed process was found to be the cause of low elastic and plastic characteristics even in the low porosity of the coating. According to the residual stress analysis, it was found that continuous deposition layers with tensile quenching stress in the Air plasma process generated a high tensile stress in the coating. For the wire arc spray, the average stress was found to be near zero. However the observed stress in HVOF and cold spray coatings was compressive due to the peening stress imparted by the high velocity spray particles.

Yilbas et al. studied laser melting of HVOF [44]. Spraying of Inconel 625 powders on mild steel work pieces was carried out. Nd:Yag laser was used to irradiate coating surfaces after applying HVOF. The mechanical properties of HVOF coating prior to and after laser treatment were examined through three point bend tests. SEM was used for morphology examinations of coating surface. It was found that the elastic limit of the laser treated coating was less than that corresponding treated coating. The holding load of the work piece with coating was much higher than that corresponding to the uncoated work piece for unknown displacement.

This showed that the (250 μm) small thickness of Inconel 625 coating enhanced the toughness of the work piece considerably. Due to the compact structure in the case of laser treatment, the shear deformation was larger. The bubbles formed during the laser melting escape, leaving small holes on the surface. The shear stress on the coating-substrate interface triggered the crack initiation at the affected site. Furthermore, the scattered splats with high oxygen content were considered as another source for initiation of crack centers due to structural brittleness. During laser treatment, the high cooling rate resulted in trapping of the gas in the melt zone, which enhanced the porosity in the surface region of coating. The presence of hemispherical protuberances after laser treatment in the outer edges of coating was observed, which indicated the existence of partially melted splats in this region.

The influence of the WC-12Co deposited by low power plasma spray ranged from (3-10 kW) on the microstructure, phase structure and hardness properties of the coatings was studied by Morks et al. [4]. The powder were sprayed on stainless steel substrate with various plasma power 3.9, 6.5, 7.8 and 9.1 kW. The power was changed by having a constant current (130 A) and varying the voltage from 30 to 70 by increasing the hydrogen gas flow rate. The coating microstructure was evaluated using EDX, XRD and SEM. In addition, the microhardness test

was carried out. It was found that spraying in low pressure led to a sufficient decrease in the hardness because of the attendance of WC particles in thick layer of soft Co binder. It was noticed the hardness of the coating increased as the plasma power increased. Due to the decomposition of coating at high flame temperature, W_2C phase took place on the obtained coating. Spraying the cermet coating with 6.5 kW power at arc current of 130 (A) and voltage of 50 (V) was recommended in order to obtain high hardness cermet coatings.

Chivavibul et al. conducted a comparative experiment of a warm spray process and HVOF in order to verify the capability of the warm spray process (WS) to be used for cermet coating [45]. The warming process was carried out by adding a mixing chamber to the HVOF equipment to lower the temperature ranges, which in turn eliminated the degradation of WC during the spraying in high temperature. Three types of WC-Co coatings with an average carbide size of 0.2 μm and various cobalt contents (12, 17 and 25 wt %) were obtained by HVOF and warm spray. X-Ray Diffraction and Scanning Electron Microscope were used for morphology examinations of the coating surface. The hardness, fracture toughness and abrasive wear properties were determined. It was shown that in WS coating hardness, Co content relation was similar to that

insintered material, whereas HVOF coating behaved differently. However, the hardness of HVOF coatings was higher than those of the warm spray. Moreover, WS coating fracture toughness increased with increasing Co content, while it had the opposite trend in HVOF coating. In addition, it was found that the wear behavior was improved in the warm spray process due to the microstructure and phase distribution in the coating. Therefore, the warm spray was evaluated as an effective technique to obtain WC-Co coating without dissolution and decarburization of WC.

An attempt of deposition WC-Co coating for the steam generation plant was done by Kauret al. using the detonation gun sprayed method [7]. The oxidation performance of detonation- sprayed WC-Co coatings at 700 °C air and in the simulated environment of boilers were investigated. It was found that detonation- gun spray was a proper way to apply WC-Co on T22 steel boiler tube material. WC-Co With compression to uncoated specimens, the WC-Co coated specimens were found to have lesser overall weight gains both environments. Moreover, Fe and O formation took place as a result of the oxidation of the substrate steel in both environments, whereas the oxidation of the coated steel in air indicated the formation of W with some significant amount of O, Fe and Co. For all

specimens, the oxidation resistance was found to be more in a salt environment.

2.6 Summary of Literature Review

In the literature, considerable researches have been performed on HVOF coatings to examine the characterization and mechanical properties of the coating. The researchers also investigated the influence of spray variables and powder morphologies on the resulting coating. However, the research was limited to specific applications. In oil and gas industries, alloy steel was used to manufacture of rotating and stationary components which were subjected to highly harsh environments. The available literature showed that much research had been reported with various types of HVOF deposited coating on alloy steel substrate. In addition, tungsten carbide/ nickel alloy as well as molybdenum blends were used as a protective coating on various steels. However, these researches showed that both of coating blends were used as a single coating layer to provide corrosion and wear protection. To the author's knowledge, there had not been many research reported in which (Diamalloy 2002) tungsten carbide cobalt/ nickel alloy blend and (Diamalloy 4010) were applied one layer over the other to obtain multilayered coating on alloy steel substrate.

Furthermore, they did not cover the details of the specific properties of HVOF coating of Diamalloy 2002 and 4010 on alloy steel substrate.

The present study was carried out to examine the mechanical properties of such coatings in details in relation to many of their applications in mechanical equipment in oil and gas industries. The literature survey was classified according to four categories. They are mechanical and chemical properties of HVOF coatings, thermal spray powder characterizations, HVOF spraying parameters affecting coating quality and thermal spray processes comparison.

Chapter 3- Experimental Equipment and Procedure

3.1 Introduction

In this chapter the equipment used and procedure adapted for the bending, tensile and hardness characterization of HVOF thermally sprayed Diamalloy 2002 and Diamalloy 4010 coatings on alloy steel substrates were presented. Each test was repeated three times for each category of specimen including HVOF coating of Diamalloy 2002 and Diamalloy 4010 as well as two-layered coatings consisting of Diamalloy 4010 and Diamalloy 2002. In the two-layered structure, Diamalloy 4010 was sprayed as a first layer on the substrate surface since Diamalloy 4010 was used to fill the cavities in AISI 4140 steel surface in repair applications. This was because of the fact that the elemental composition of Diamalloy 4010, which was almost similar to AISI 4140 steel. Diamalloy alloy 2002, then, was applied as a second coating for the wear and corrosion protection of the surface due to presence of carbides in the powder.

3.2 Sample Preparation

Steel is the most common material used in the oil and gas industrial where it is usually subjected to the harsh environment such as high temperature, corrosion and wears environments. Therefore, AISI 4140 was selected as the workpiece. The elemental composition (wt %) of AISI 4140 is [Fe97.25Cr1.00Mn0.85C0.40Si0.25Mo0.25]. AISI 4140 alloy steel is suitable for a variety of applications in the oil and gas sector. [46]

The specimens were classified, in terms of geometry. The first category of the specimens had curvatures in the region close to the grip holders which had radius between ends. The presence of curvatures in the first category samples was in line with ASTM standard for tensile specimens [47]. The second category of the specimens with rectangular bar was used for three-point bending tests shown in Figure 3.1. The specimens with a radius between ends were of dimensions of 140 x 15 x 3 mm, while the rectangle bar specimens were of dimensions of 140 x 20 x 3 mm, in relation to ASTM standard for tensile specimens [47].

3.3 Surface Treatment

Since the quality assessment was part of this investigation, the surface modification was extremely essential to enhance and improve the adhesion of the coating [48]. Grit blasting was carried out to roughen the surface, which in turn, removed and cleaned any contamination at the surface of the substrate prior to spraying. Moreover, a sufficient enhancement in the bond strength between the deposited coating and substrate surface was resulted by applying the grit blasting to the substrate surface [29]. The grit blasting process was conducted to all specimens using 20 mesh Al_2O_3 particles at pressure of 550 kPa to roughen the surface for three minutes. The grit blasted surfaces had roughness on the order of 50 - 60 μm . The specimens were cleaned once more by compressed air prior to apply the desire coating. The HVOF thermal spraying was applied directly after grit blasting process to avoid moisture contamination. A grit blasting machine manufactured by Empire Company was employed to perform the grit blasting process as shown in figure 3.2.

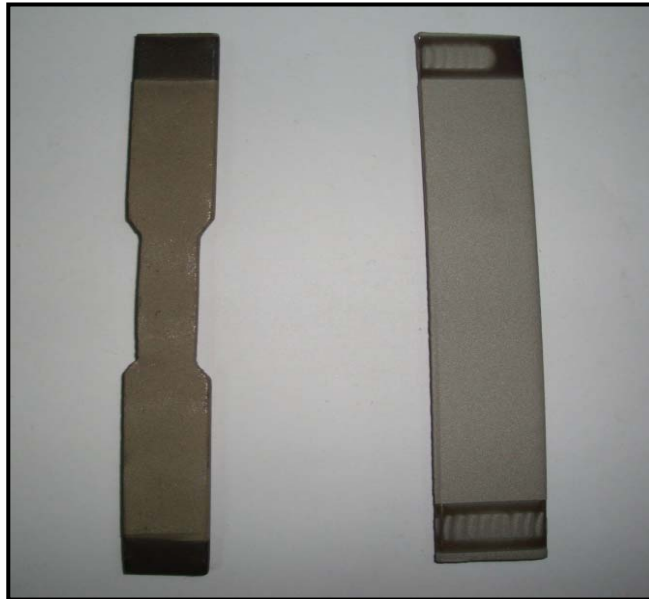


Figure 3.1 Photograph of the two types of specimens used in the tests



Figure 3.2 Grit blasting machine

3.4 HVOF Thermal Spraying System

3.4.1 Powder Materials

Both of Iron/molybdenum blend (Diamalloy 4010) and tungsten cobalt carbide/nickel alloy blend (Diamalloy 2002) manufactured by Sulzermetco company were used in the current experiment.

Diamalloy 4010 with a particle size of $45 \pm 5.5 \mu\text{m}$ is used as a excellent alternative of hard chrome plating used for surface protection, against abrasive grains, wear and fretting. Moreover, Diamalloy 2002, with $45 \pm 11 \mu\text{m}$ parical size, had superior wear and corrosion properties up to 540°C . The chemical composition of the coating powders is given in table 3.1.[5]

Table 3.1 Chemical composition of the coating powders (wt %).[5]

Powder Material	Moroplogy	Chemical Composition						
		Fe	Mo	Cr	Mn			
Dimalloy 4010	Blend	68	30	1.8	0.2			
		WC12Co	Ni	Cr	Fe	Si	B	C
Dimalloy 2002	Blend	50	33	9	3.5	2	2	0.5

3.4.2 HVOF Equipment

In this study, the high velocity oxy-fuel spray system was Sulzer Metco Manual Hybrid Diamond Jet, which worked with a propane, was employed to produce the coating on the alloy steel substrate (Figure 3.3). This HVOF system was provided with DJ9H-Hand held gun as shown in figure 3.4, 9MP-DJ powder feed rate control as well as DJFW precession flow meter.

The Sulzer Metco HVOF spraying process uses Fuel and O₂ to produce the required high kinetic energy with a certain temperature in the gun nozzle. The coating powder was fed into the gun hot zone and heated to molten and semi-molten by the hot gas stream which generates from the combustion reaction of the oxy-gen fuel mixture. A compressed air (as used in this research) was used as a coolant for the gun to prevent melting of the internal parts of the gun.

The spraying parameters for the HVOF coatings used in this work are given in table 3.2.

Table 3.2 Experiment spraying parameters

Spray Parameters	Oxygen Pressure (kPa)	Fuel pressure (kPa)	Air pressure (kPa)	Powder feed rate (m ³ /h)	Spray rate (kg/h)	Spray distance (m)
Value	1034	590-620	720	0.85	6.5	0.31



Figure 3.3 HVOF Process

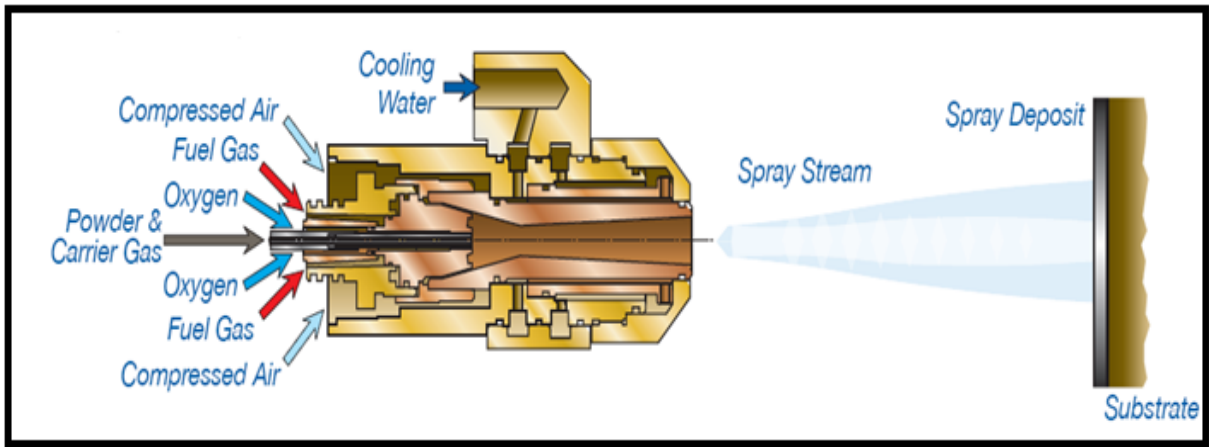


Figure 3.4 Gas Fuel HVOF Gun [5]

3.4.3 Experimental Matrix

In order to evaluate the properties of coating consisting of combination of the layers produced by different powders, three sets of test specimens were prepared. These are: HVOF coating of Diamalloy 2002 and Diamalloy 4010 as well as two-layered coatings consisting of Diamalloy 4010 (bottom layer) and Diamalloy 2002 (top layer) as illustrated in figure 3.5. All the samples tested were AISI 4140 steel. The total of 30 samples were manufactured for the tests; in which case, 10 samples were coated incorporating all powders for the sets of mechanical tests such as hardness, bending and tensile tests. The samples prepared for tensile test were one side coated, where the both sides of samples were coated for three-point bending test. Compared with single-side coated specimen, that double side coated specimen seem to have better accuracy [49]. Table 3.3 shows the prepared test samples in details. The coating thickness was measured to be about 300 μm for all test samples.

Table 3.3 The test specimen used in the study

Set	Powder	Morphology & Hardness	Tensile Test (One coated side)	Bending Test (Two coated sides)	Total of Samples
A	Diamalloy 4010	4	3	3	10
B	Diamalloy 2002	4	3	3	10
C	Diamalloy4010 (bottom)& 2002 (Top)	4	3	3	10

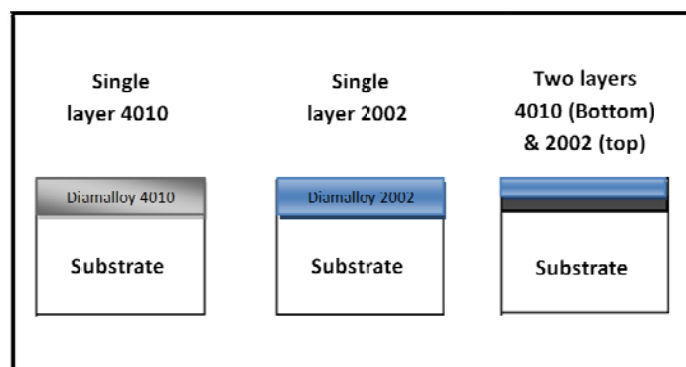


Figure 3.5 The three sets of the tested samples (single coated side)

3.5 Mechanical Tests Preparation

3.5.1 Three Point Bending Test

Three point bending tests were carried out using an INSTRON 8801 mechanical testing machine with accordance to the ASTM D 790 international standard [50]. The coated rectangular sample was tested by placing it on two supported beam on the two outer points and then applying the load downwards in the mid way between the supports by the third the central load. The specimen was deflected until rupture occurred in the outer surface of the test specimen or until a maximum strain of 5% was reached.

Three samples of each category were positioned on a three point bending support fixture to be tested. During the tests, the load and displacement characteristics were recorded. The load (P) for each test was recorded, and the bending strength (σ_b) of the all tested specimens was calculated by formula given below [50]:

$$\sigma_b = \frac{3PL}{2bd^2} \quad (3.1)$$

where P= break load, L= span, b= sample with width and d= sample thickness.

The photograph of a workpiece after the three-point bending test is shown in figure3.6.



Figure 3.6 Workpiece after the three-point bending test

3.5.1.1 Determining Young's Modulus by Three Point-Bending

The Formulation of Young's modulus was given in the previous study [51], therefore, only the governing equations would be presented. After

assuming the symmetry during the bending test in relation to figure (3.7), the Young's modulus could be written as [52]:

$$2E_c I_c + E_s I_s = \frac{Pl^3}{48d} \quad (3.2)$$

Or

$$E_c = \frac{1}{2} \left[\frac{Pl^3}{(48d)I_c} - E_s \frac{I_s}{I_c} \right] \quad (3.3)$$

where I_s and I_c are the 2nd moment of area of the substrate material and the coating, the elastic modulus of the substrate $E_s = 2.1 \times 10^{11}$ (Pa), P is the applied load (N), l (m) is the distance between the supports, and d (m) is the displacement of the substrate material and coating during the bending tests. The moments of area are:

$$I_s = \int_{-\frac{h_s}{2}}^{\frac{h_s}{2}} y^2 b dy \text{ and } I_c = \int_{-\frac{h_s}{2}}^{(\frac{h_s}{2})+h_c} y^2 b dy \quad (3.4)$$

where b is the width of the substrate material and the coating.

The load-displacement data in the plastic region was used to compute the stress relaxation rate. Table 3.4 gives the geometric data used in the simulations.

Table 3.4 Data used in calculating of Young's modulus from three-point bending test.

	h_s (m)	P (N)	h_c (m)	l (m)	b (m)	d (m)	I_s (m ⁴)	I_c (m ⁴)
Diamalloy 4010	0.003	1500	0.0003	0.08	0.02	0.003	4.5×10^{-11}	2.05×10^{-12}
Diamalloy 2002	0.003	1400	0.0003	0.08	0.02	0.002	4.5×10^{-11}	2.05×10^{-12}

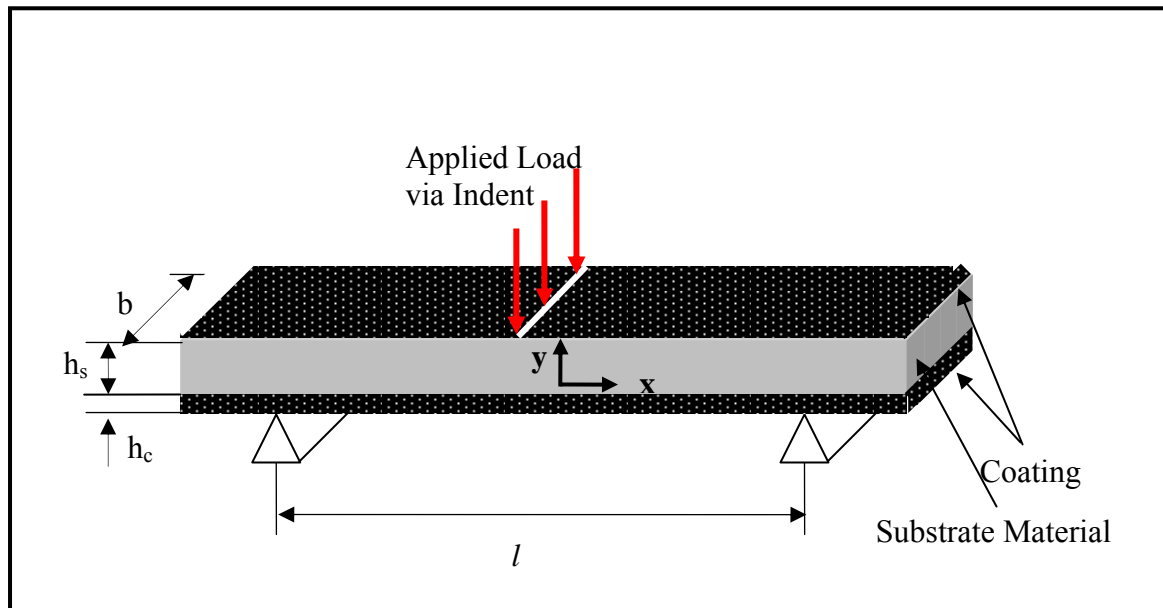


Figure 3.7 A schematic view of three-point bending testing

3.5.2 Tensile Test

The tensile test is one of the most common types of mechanical stress-strain tests performed on material. Tensile tests can be used to ascertain several mechanical properties. The recorded data from the tensile test was used to determine the elastic limit, elongation, modulus of elasticity, proportional limit, and reduction in area, tensile strength, yield point, yield strength and other tensile properties. Procedures for tensile tests of metals were given in ASTM E8 [47]. This standard procedure was for tension testing of metallic material under uniaxial tensile stress at room temperature, specifically, the methods for determination of yield strength, yield point elongation, tensile strength, elongation and reduction of area.

Tensile testing was performed on an Instron 8801 (Figure 3.8) testing system which is capable of doing a wide variety of mechanical tests. Instrument control (including standard and customizable methods) and data collection and analysis were performed through Instron's Bluehill software. The setup was equipped with an environmental chamber that allowed testing over a wide range of highly controlled temperatures for conducting tensile tests.

The test specimen was mounted by its ends into the holding grips of the testing apparatus. The elastic modulus was obtained by getting the load and both position data throughout the test. The maximum stress value just before fracture was selected as the tensile strength and the final actuator

position gave the fracture point. The tensile tests were conducted at a cross head speed of 2 mm/min. Minimum of 3 specimens was tested for each condition. The error related to the tensile tests was estimated as 3%. Figure 3.9 shows the work piece after the tensile test.

$$\sigma_a = \frac{P}{A_m} \quad (3.5)$$

where, P is the maximum load and A_m is the minimum cross sectional area.

The standard error was estimated from:

$$\sigma_{est} = \sqrt{\frac{\sum(x-\bar{x})^2}{N}} \quad (3.6)$$

where \bar{x} is the mean value of the response measured, x is the value of the measured response and N is the number of data points.



Figure 3.8 The Tensile test machine [53]



Figure 3.9 A photograph of work piece after the tensile test

3.5.3 Vickers Indentation Test

The Vicker's indentation tests were carried out to estimate the hardness of the coating as well as young's modulus. Indentation testing is a mechanical testing process designed to determine the properties of material by applying the indenter at the surface of a sample. Surface indentation have long been the domain of hardness testing. Vickers is traditional indentation hardness test that was carried out to estimate the plane fracture toughness of the coating.

The test was performed by Indentation Hardness Tester manufactures by Buehler Company. (Figure 3.10). In this case, microhardness in HV and crack length generated due to indentation at the surface was measured using 20 N load on mounted cross sections of coated samples. The specification of the indentation hardness tester is shown in table 3.5.

Table 3.5 Specification of indentation hardness tester

Model	Manufacturer	Specification
5112	BUEHLER	<ul style="list-style-type: none"> ➤ Force range of 2N to 200N ➤ Two Objectives and a Vickers Indenter Mounted on a Motorized Turret ➤ Large Easy-To-Use LCD console for tester control and hardness readout ➤ Precision Digital Filar with 0.1µm Resolution ➤ Powerful Halogen Illuminator.



Figure 3.10 Indentation test equipment

3.5.3.1 Determining Young's Modulus by Indentation Test

The elastic response of the surface when subjected to indentation test needed to be considered in order that the Young's modulus could be determined. After considering Figure (3.11), the Young's modulus could be formulated as [53]:

$$E^* = \left(\frac{9}{16}\right)^{0.5} P . h^{-1.5} . R^{-0.5} \quad (3.7)$$

where P is the applied load, h is the elastic penetration of the indenter and R is the equivalent radius. The true modulus of elasticity could be determined using the indenter properties [55]:

$$E = \frac{1 - \nu^2}{\frac{1 - \nu_i^2}{E_i} + \frac{1 - \nu^2}{E^*}} \quad (3.8)$$

where E_i and ν_i were the Young's modulus and Poisson's ratio of indenter, respectively. In the calculations $E_i = 1141$ and $\nu_i = 0.07$ (diamond indenter) and $\nu = 0.278$ (coating material) were taken [55].

The indentation tests were repeated minimum of three times and the error estimated from the experimental data for the particular test was determined as 8%.

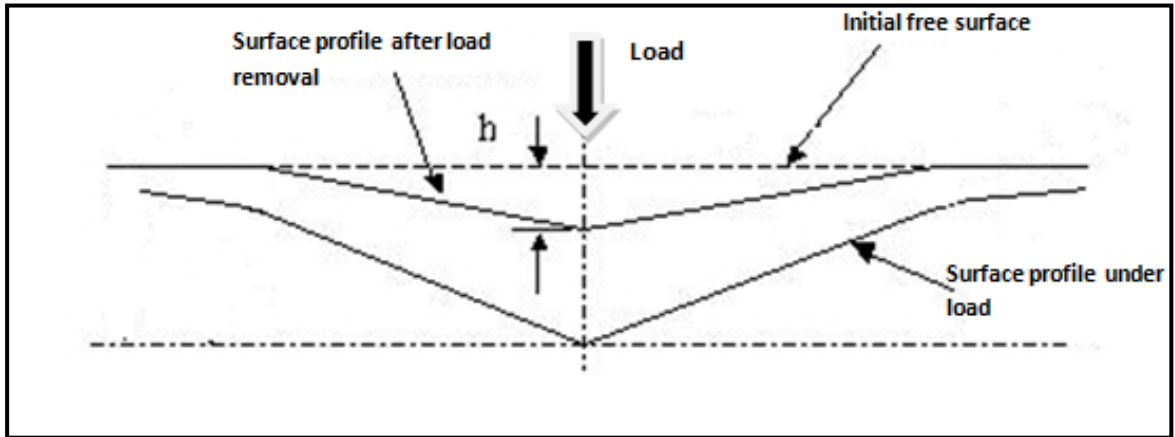


Figure 3.11 Schematic view of indentation and relevant dimensions

adapted from [56]

3.6 Metallographic Preparation

Metallography was the technique of taking image for topographical or microstructural features on prepared surfaces of materials. The properties and performance of coating materials may be controlled by studying the microstructures using metallography. Metallographic specimen preparation was an important tool for the characterization of thermally sprayed coatings in terms of revealing the coating/substrate interface, coating layer morphology and location. The metallographical process could be divided into four different stages; sectioning, mounting, grinding and polishing.

3.6.1 Sectioning

Sectioning was a necessary step before the mounting to reduce the size of test samples or to explore its hidden cross-section. The test specimens were sectioned using a Labotom-3 cut off machine manufactured by Struers (figure 3.12). Cooling water was applied directly cut-off wheel resulting in an excellent cooling of the cutting area. The speed of on cut-off wheel was 3450 rpm.

3.6.2 Mounting

In the current research, hot mounting technique was selected to mount the samples. Hot mounting uses both heat and pressure to thermoset resin. This method, in some cases, was not preferred particularly if the sample had a loose layer on its surface. However, in the thermal spray deposits case the coating had adequate adherence to its substrate, hence it was not affected by the hot mounting. In hot-mounting the sample was surrounded by an organic polymeric powder (thermoset resin) which melts under the influence of heat (up to 200 °C). Pressure was also applied by a piston, ensuring a high quality mould free of porosity and with intimate contact between the sample and the polymer.

The hot mounting process SIMPLIMET 2000 made by BUEHLER (Figure 3.13) was used to mount different types of coatings and powder samples.

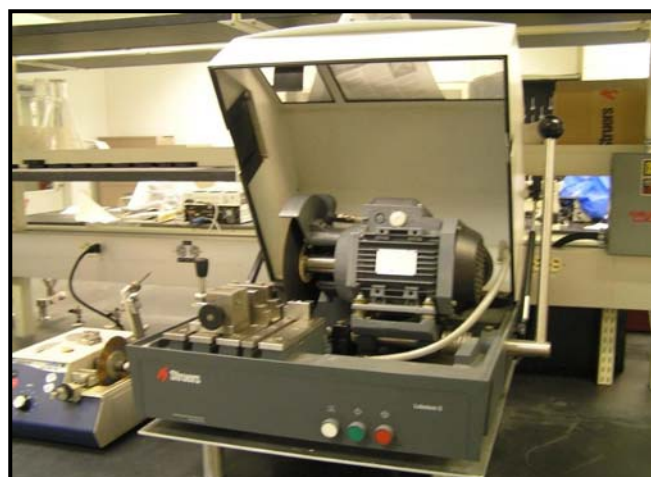


Figure 3.12 Cut-off machine



Figure 3.13 Mounting machine

3.6.3 Grinding and Polishing

The prepared mount (sample contained in a thermoset mould) was then subjected to a series of grinding and polishing steps, with the aim of producing a surface which would revealed its microstructure characteristics. The StruersLaboPol 5 machine (Figure 3.14) was used to grind and polish the samples, automatically. Automation of grinding and polishing stage was essential as it eliminated operational error such as

applied load and rotation per minute The procedure of preparing the sample was consisted of four steps; plane grinding ,fine grinding, fine polishing and final polishing.[57]

3.6.3.1 Plane Grinding

The purpose of using plane grinding was to remove the damage due to the sectioning stages and to produce a flat plane for subsequent grinding. A fine Silicon Carbide paper (SiC-paper 220) was initially used to remove all damage without introducing new damages in the coating. The water was used as lubricant and the contact pressure was 180 N. The speed of the grinding process was 300 rpm.

3.6.3.2 Fine Grinding

The fine grinding step was performed to retain and assure with the removing the damage caused by the plane grinding. MD-Largo paper and and DiaPro Allego Diamond suspension was used at this step of the grinding. The duration of fine grinding step was 5 minutes under 180 N contact force with 300 rpm.

3.6.3.3 Fine Polishing

The objective of the polishing stage was to remove any smearing or deformation which had taken place in previous grinding stage. In the current research, MD-Dac polishing surface was used for duration of 5minutes to prepare the coated specimens. Polishing was performed for 5 min at a contact pressure of 180 N with 150 rpm. DiaPro Dac was selected as a suspension.

3.6.3.4 Final Polishing

The polishing duration of this final stage was 1 minute using MD-Nap as polishing surface and DiaProNap B as suspension where the contact force was 120 N with 150 rpm.



Fig 3.14 LaboPol 5 used for grinding and polishing

3.7 Characterization Analysis

3.7.1 Optical Microscope

The optical microscope equipment that was used in this study was manufactured by Olympus as shown in figure 3.15. It was Olympus BX

60 optical microscope with Ploaroid digital microscope camera (DMC) attached to it. It was used for microscopic observation and to obtain optical micrographs of the surface. The microscopic had revolving nosepieces with 5 objective lenses of various magnifications attached to it. The magnification levels were 50X, 100X, 200X, 500X and 1000X.

3.7.2 SEM and EDS Techniques

The microstructural and elemental characterization of the powder and cross sections of the deposited coatings were investigated using Scanning Electron Microscopy (SEM) equipped with Energy Dispersive Spectroscopy (EDS) and using optical microscope. The tests were

performed using JEOL JDX- 3530 with specifications of resolution 3.0nm, accelerating voltage 0.3 to 30 kV and magnificationx5 to 300,000 as shown in figure 3.16.

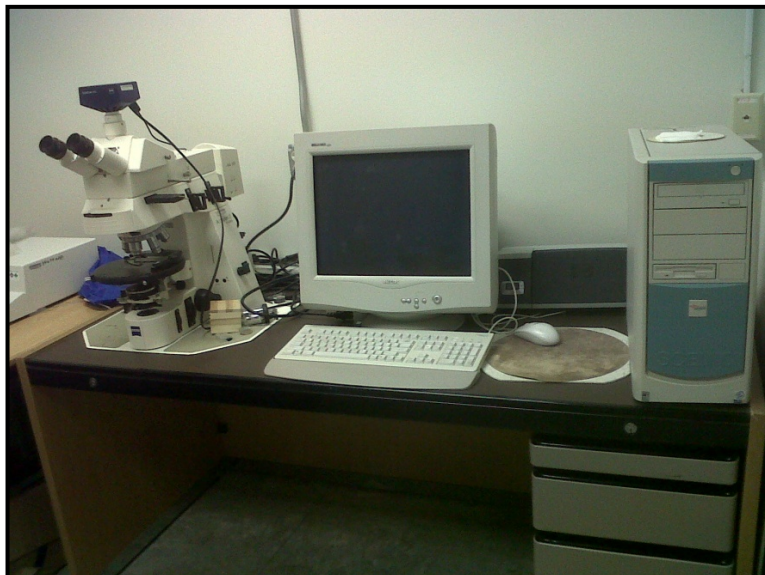


Figure 3.15 Optical Microscope

Figure 3.16 Scanning Electron Microscopy (SEM)

Chapter 4- Results And Discussion



4.1 Introduction

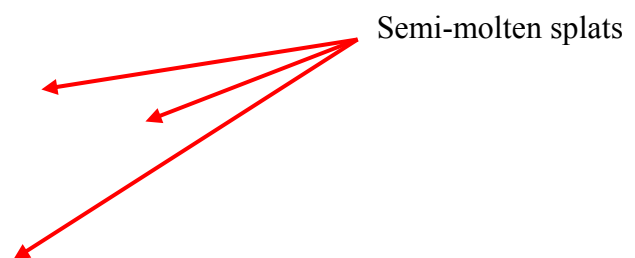
The aim of this chapter is to discuss the results of the experimental study of HVOF spraying of powders composing of iron/molybdenum blend as well as tungsten carbide cobalt/ nickel alloy blend onto alloy steel sheets. The mechanical and metallurgical properties of the single and two layered coatings were investigated. The behavior of the coating material under the mechanical tests, indentation test, three point bending test and tensile test were evaluated.

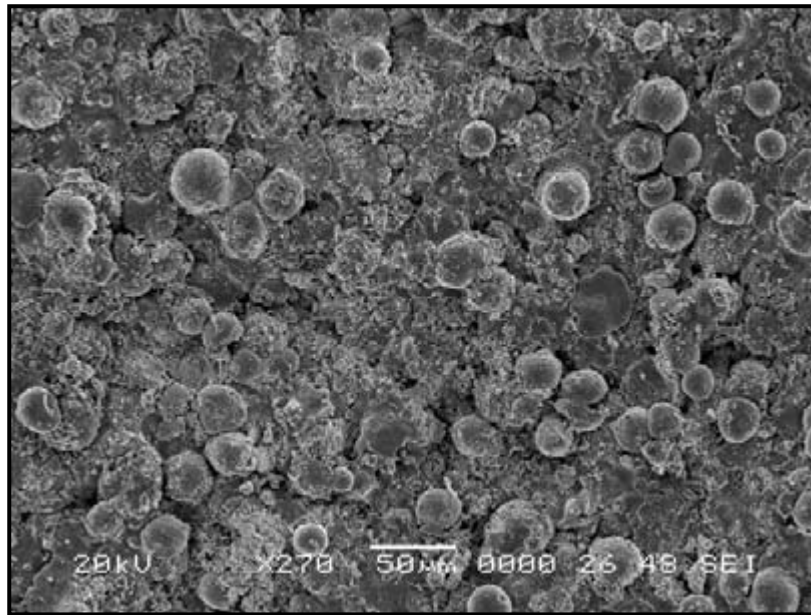
4.2 Microstructure Examination

HVOF coating of two-layers consisting of Diamalloy 4010 and 2002 powders deposited onto alloy steel was carried out. The surface morphology and microstructure of the coating were examined using SEM. Elastic modulus of each layer was measured using the indentation method.

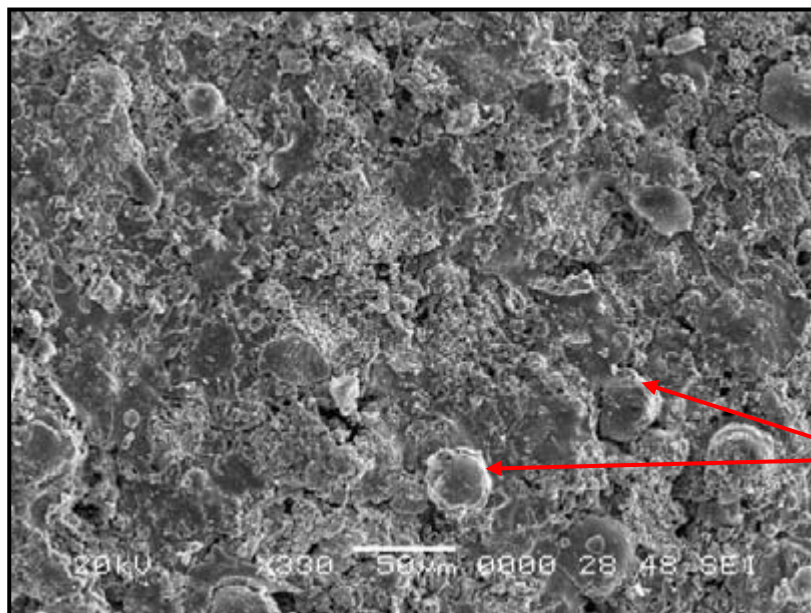
Figure 4.1 shows SEM micrographs of the top view of the coatings produced by Diamalloy 4010 and 2002 powders it was evident that no large loose splats and surface irregularities including voids, cracks and cavities were observed. However, surface roughness was high because of the presence of the partially molten powders. The surface roughness profile was shown figure 4.2. This was true for the surfaces resulted from

both powders. It should be noted that Diamalloy 2002 contained WC, which had a high melting temperature. Consequently, the molten state of the powders required excessive temperature rise during the spraying process. This could also be observed from the SEM micrographs, i.e. some protruded particles were observed. Moreover, high spraying velocity increased the momentum of the particles and, upon impacting, some particles penetrated into the coating surface. Consequently, the protruded particle distribution was random and they cover a small area at the coating surface.





(a) Diamalloy 2002 Coating



Semi-molten splats

(b) Diamalloy 4010 Coating

Figure 4.1 SEM micrographs of top view of coatings produced from Diamalloy 2002 and Diamalloy 4010 powders.

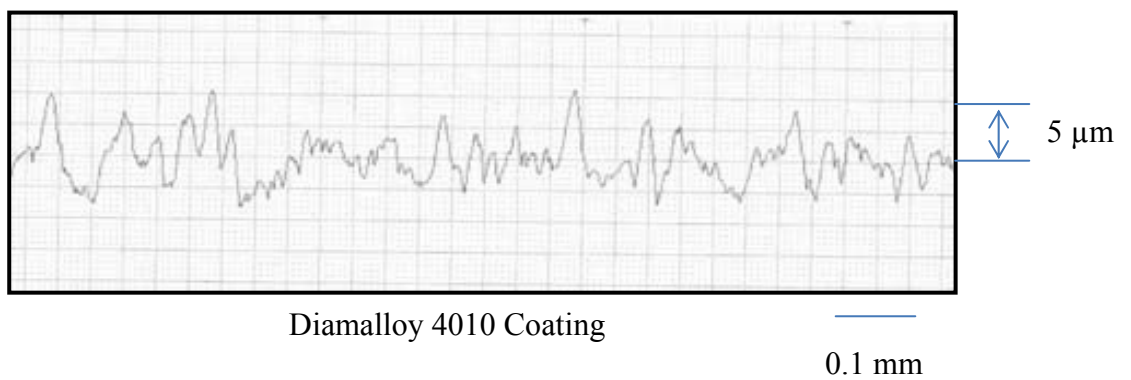
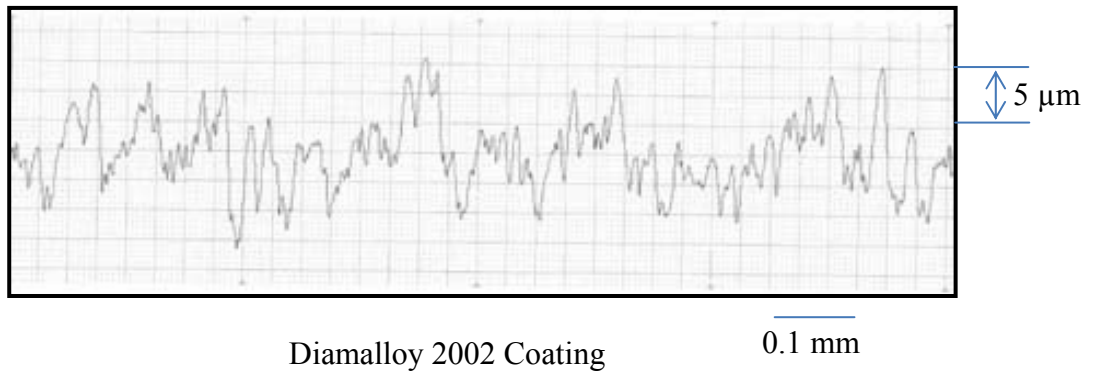


Figure 4.2 Roughness of the coating surfaces

Figure (4.3 a and b) shows SEM micrographs for the cross-section of the coatings including single layer coatings produced from Diamalloy 2002

and 4010 powders as well as the two layered coating. It should be noted that the top layer was produced by using Diamalloy 2002 in two layered coating. It was evident that the coating consists of lamellar structure, which was produced during the multi-pass spraying process. Moreover, the porosity in the coating was measured using the SEM micrographs and the optical image analyzer. It was found that the porosity was in the order of 3 %. The possible cause of the porosity was due to the presence of the semi-molten and molten splats during the spraying process as well as uneven shapes of the powders. The presence of semi molten and hard splats was evident and they appear as rounded shapes in the coating; however, this was mainly observed in the surface region of the coatings, particularly for 2002 Diamalloy coating. This was because of the presence of WC in the powders, which required high temperature for melting. Moreover, some stringers like inclusions were also observed in both coatings. This may be attributed to the oxide formation during the spraying process, i.e. high temperature oxidation occurred around the splats during the spraying process as also observed in the previous study [58]. This situation could also be seen from the EDS line scan, which was shown in figure 4.4. The presence of O₂ showed that oxidation took place around the splat surface, provided that the oxide layer may not cover the whole surface. This situation was true for both coating produced using

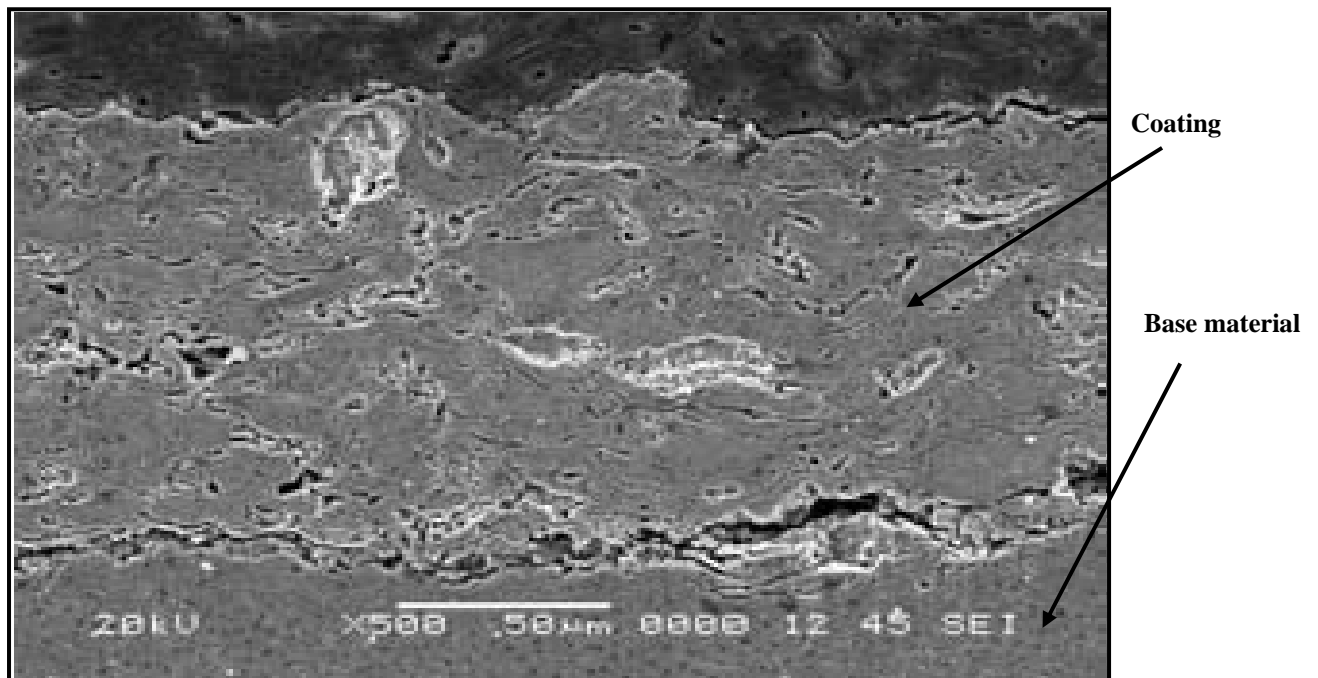
Diamalloy 2002 and 4010 powders. The splats were well integrated into the base material at the coating base material interface. No large cavity or other irregular structure was observed. This indicated that the high velocity of the molten splats were widen over the surface upon high velocity impact. This was particularly true for the coating produced from Diamalloy 4010. In the case of Diamalloy 2002 coating, a small gap of discontinuity was observed at the interface between the coating and the base material, provided the gap was not extended to large area at the interface. This may be because of the presence of WC, which remained at solid phase during the spraying process due to its high melting temperature.



← Coating

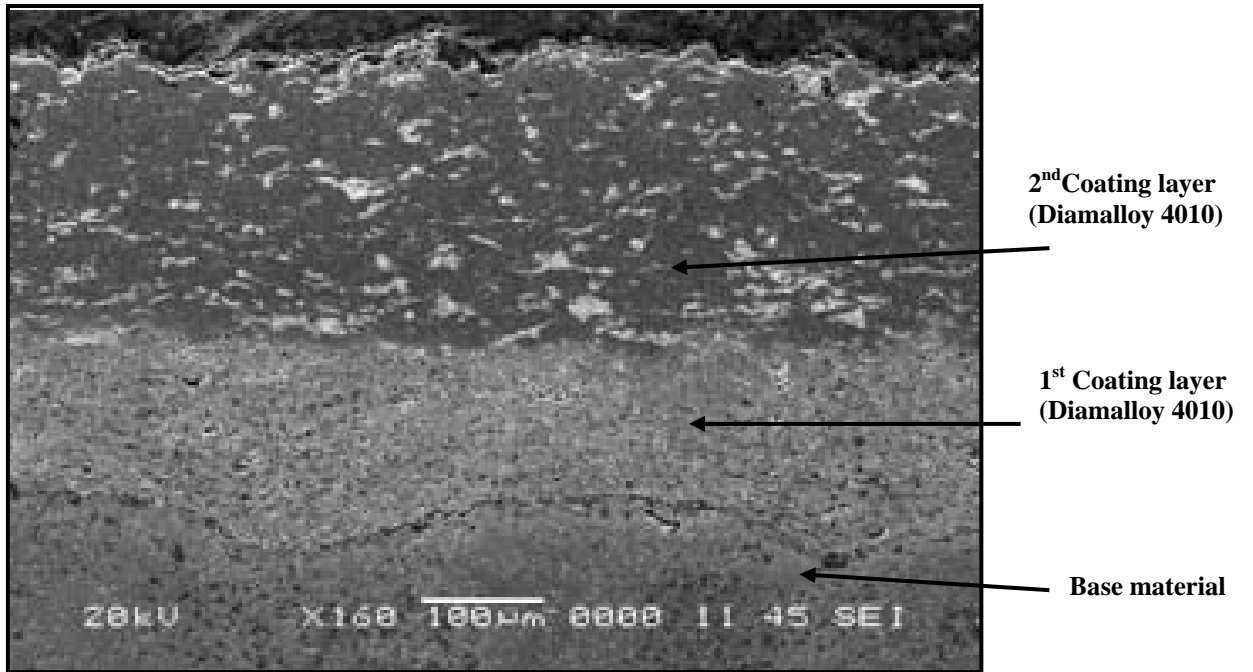
← Base material

Diamalloy 2002



Diamalloy 4010

Figure 4.3 (a) SEM micrographs of cross-sections of single layered coating



Diamalloy 4010 and 2002

Figure 4.3 (b) SEM micrograph of twolayered coatings with two different powders.

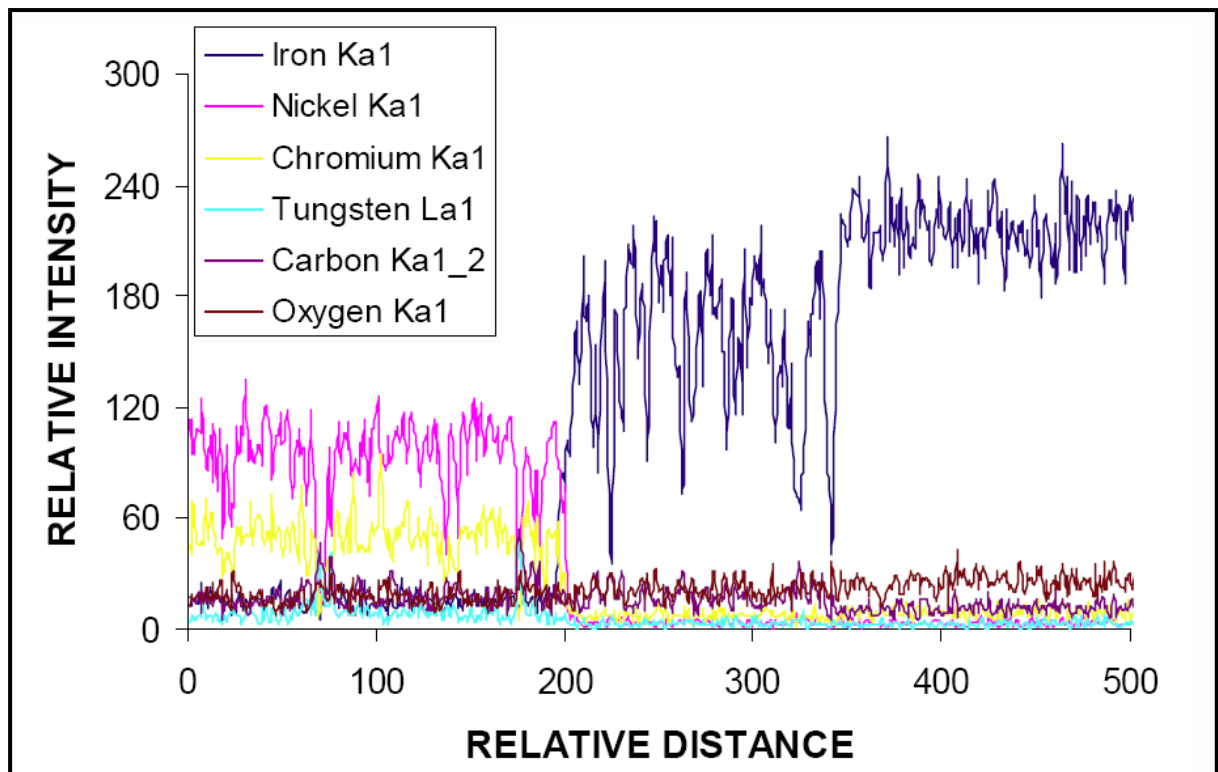


Figure 4.4 EDS line scan at the top surface of the Diamalloy 2002 coating.

Figure (4.5) shows indentation marks produced at the surface of Diamalloy 2002 and 4010 coatings as well as in the cross sections. It was

evident the marks produced in Diamalloy 2002 coating was smaller in size than that corresponding to Diamalloy 4010. This was because of the hardness of the Diamalloy 2002 coating due to the presence of WC powders. Moreover, only small cracks were observed around the indentation marks. This was true for all the coatings. The formation of the small size cracks around the indentation marks was unable to determine the surface fracture toughness. However, the fracture toughness may vary over the coating surface despite the fact that the measurement covered the layer area at the surface. Moreover, the cracks produced around the indentation marks were mainly along the direction of lamella structure, which was parallel to the coating surface. This was because of the direction, which was most prone to decohesion (easiness of delamination). This situation was observed from the indentation marks produced at the coating cross sections. It should be noted that the absence of reasonably large radial cracks did not show the low fracture toughness; however, low tensile strength of the coating. In this case, sharp edge of indenter resulted in large tensile stresses around the indentation marks [59].

Table 4.1 gives the elastic modulus determined from the indentation tests for all the coatings. It was evident that the elastic modulus for the coating

produced from Diamalloy 2002 powders was higher than that corresponding to Diamalloy 4010. This was because of the high surface hardness of Diamalloy 2002 coating. It should be noted that the error related to the measurement was in the order of 8%. Since the elastic modulus measurement was limited with the surface, two layers coating resulted the surface elastic modulus similar to that of Diamalloy 2002. This was because of the top layer in the coating, which was Diamalloy 2002. In addition, the stress developed in two layer coating was compressive because of it was large thickness. Consequently, for proper assessment of the elastic modulus, further tests were needed, such as three point bending and tensile tests.

Table 4.1 Data obtained after indenting tests for the coating

	E (GPa)	E* (GPa)	h (μm)	R (μm)	P (N)	(HV)
Diamalloy 2002	54.6	56.3	9	40	20	690
Diamalloy 4010	44.1	45.9	10	60	20	540

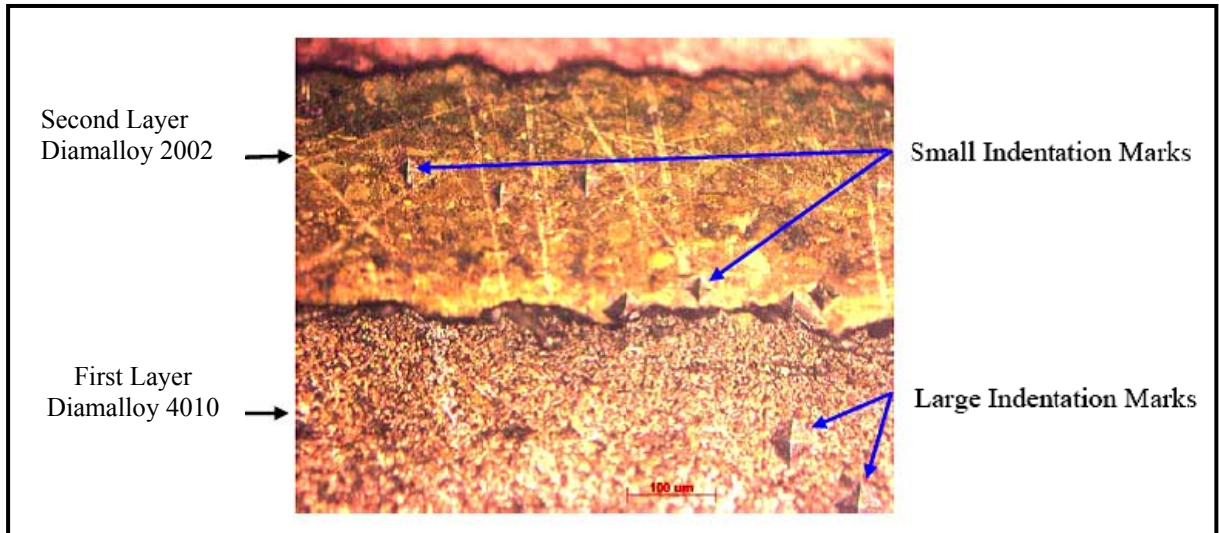
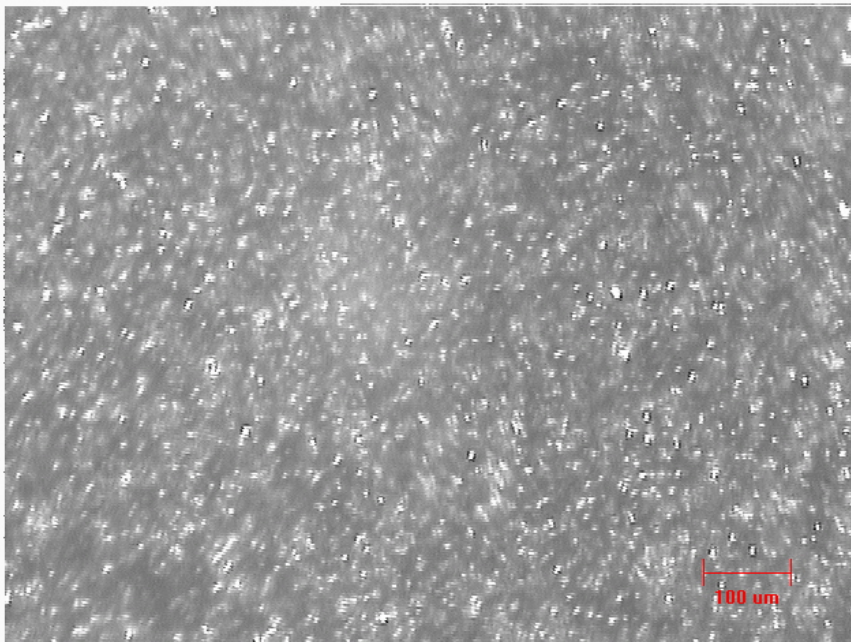


Figure 4.5 Optical photographs of indentation marks across the two layered coating

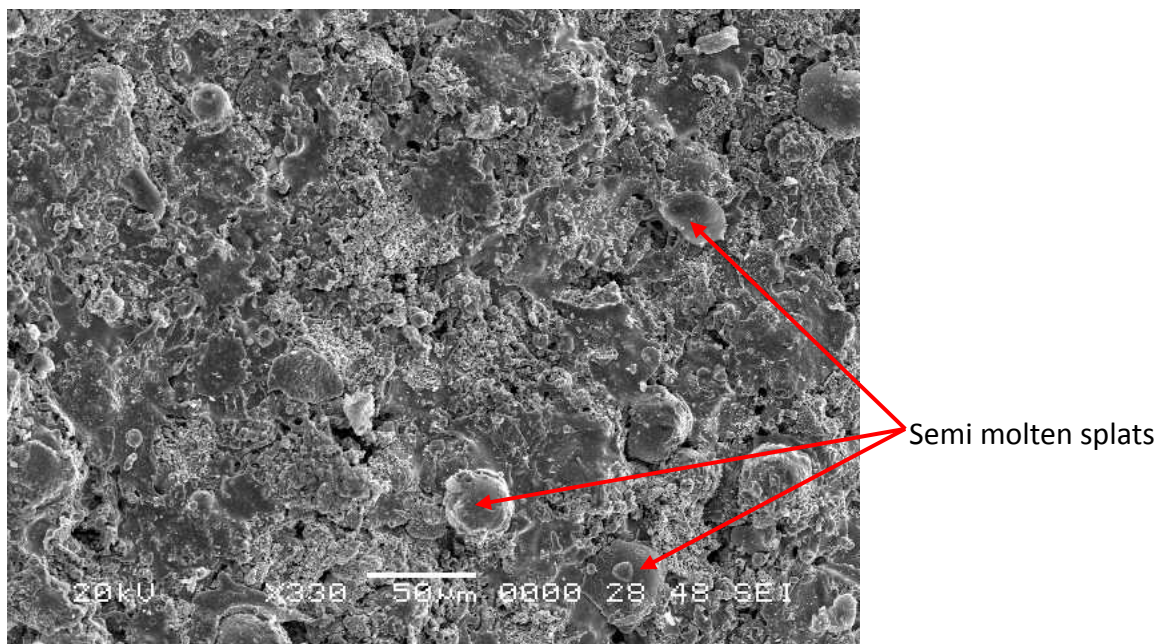
4.3 Tensile and Bending Response of Coating

The mechanical properties of the resulting coatings were examined through tensile and three-point bending tests. Figure 4.6 shows optical and SEM micrographs of the top surface of the coatings, while figures 4.7 and 4.8 show the cross section of the single layered coatings and two-layered coating, respectively. It was evident for the SEM micrograph that no large loose splats or surface asperities such as cavities or cracks were observed at the top surface of the coating. The micrographs for cross-section of the coating showed that lamella like structure was formed due to the presence of molten state of splats on set of impacting the surface. However, locally scattered spherical splats were also evident. This indicated the presence of semi-molten state of some splats. However, they appeared to be few in number. Moreover, the presence of the dark inclusions (stringers) in the surface region of the coating was evident. This indicated the presence of oxide particles with small size, which was attributed to oxidation of small particles during in-flight. The similar structure was also reported in the previous study [60]. However oxidation of the splats at coating surface after the impacting also contributes to the oxidation state of the coatings. The splat size had significant effect on the oxidation process, in which case, oxygen content increased as the particle size reduced [58]. The splat size changed for Diamalloy 2002 due to the presence of WC, which was 12%, in the coating. The porosity of

Diamalloy 2002 coatings was higher than that of Diamalloy 4010. This was because of the presence of solid phase WC particles, which did not integrate with neighboring splats in molten state.

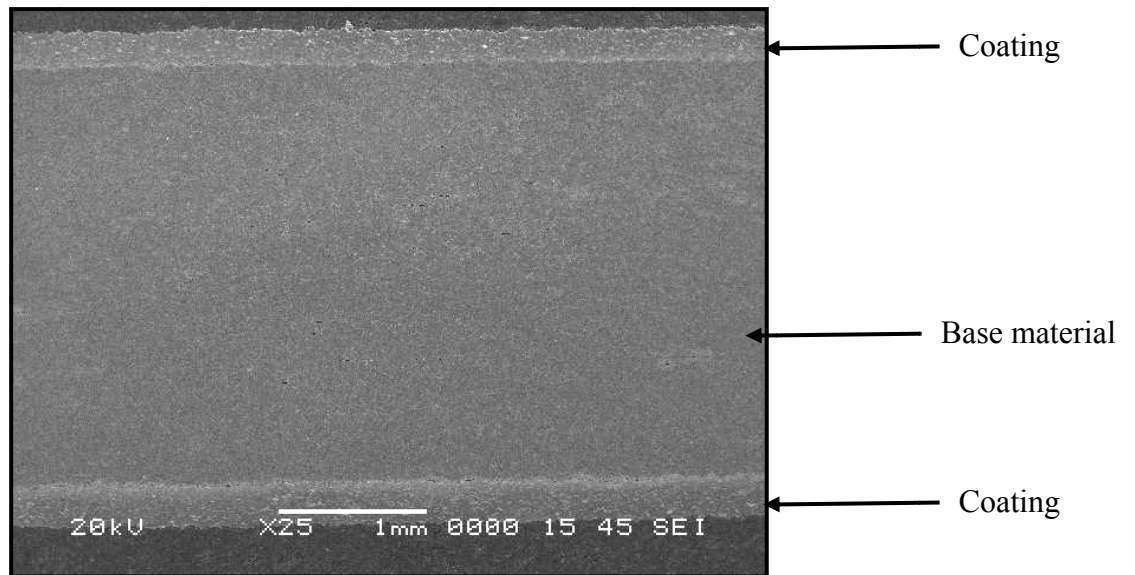


Optical Micrograph of top surface

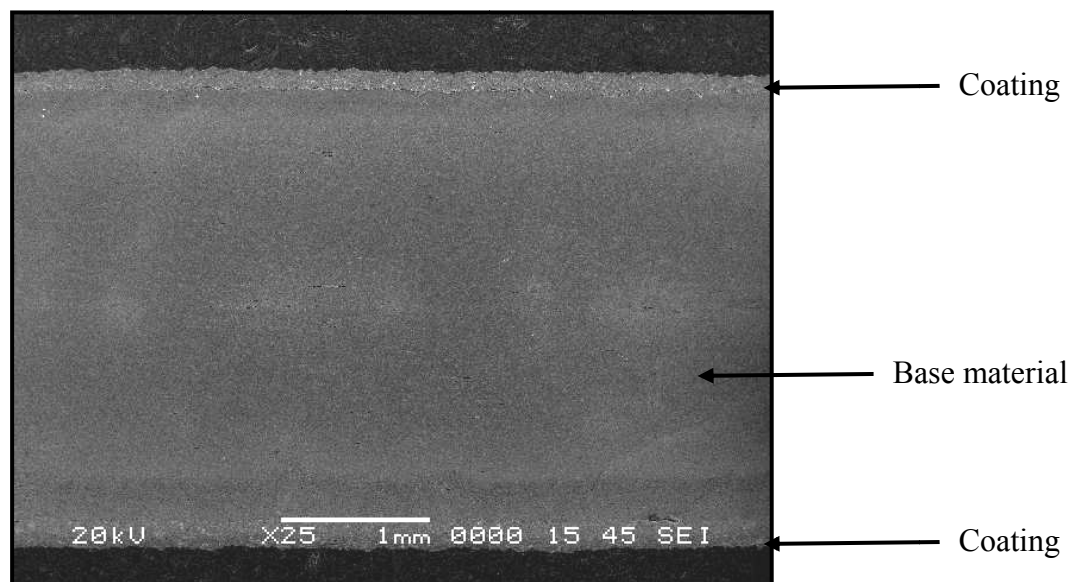


SEM micrograph of top surface

Figure 4.6 Optical and SEM micrograph of Diamalloy 2002 HVOF coated surface



Diamalloy 2002



Diamalloy 4010

Figure 4.7 Cross-sections of the single layer HVOF coated workpiece

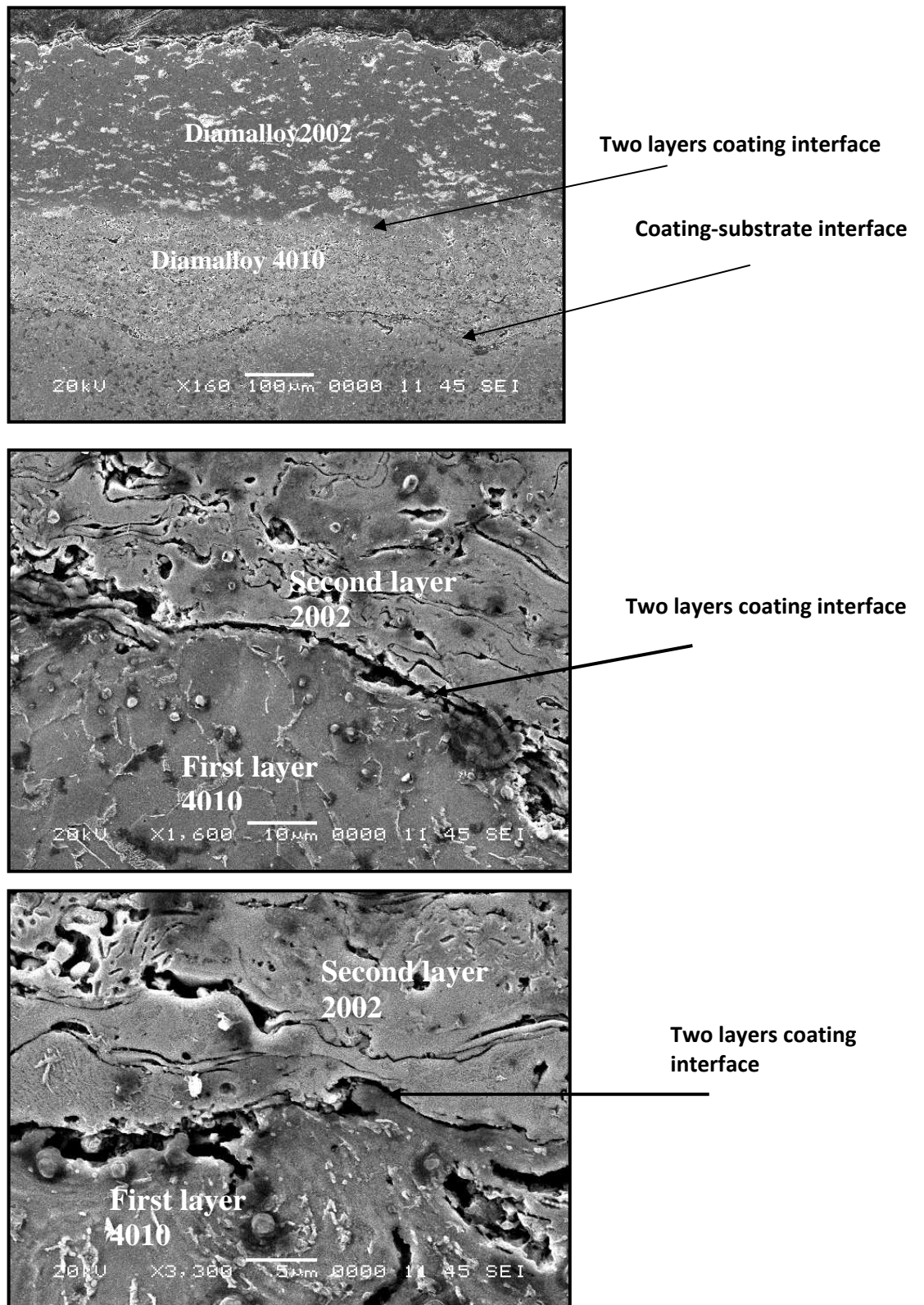


Figure 4.8 Cross-sections of the two-layered HVOF coated workpiece.

Figure 4.9 shows tensile test results for coating produced from Diamalloy 2002 and Diamalloy 4010 for single as well as for two layers. In general, stiffness increased slightly for coating produced using Diamalloy 4010. The elastic limit of the coating increased for Diamalloy 4010 and two layered coating. It should be noted that oxide formation around the splats contributed to the stiffness and elastic limit of the coatings. However, coating produced using Diamalloy 2002 powders and two layered structure had similar stress-strain behavior almost up to the elastic limit. This indicated that the influence of Diamalloy 2002 on the tensile behavior was more pronounced. Moreover, the smooth variation of stress-strain curve up to the elastic limit indicated that tensile loading did not produce excessive number of cracks affecting the tensile behavior of the coated workpiece. However in the region of the elastic limit, irregularities in the form of broken lines in the tensile curve indicated the formation of cracks in the coating. This was particularly true for two-layered coating. In this case, the stress developed at interface of first and second layers in the coating initiated the cracks in the coating. When the coating was fractured under the tensile load, the stress relaxation occurred in the coating; in which case, the energy was dissipated through the cracks and secondary cracking with increasing tensile load cease.

Figure 4.10 shows SEM micrographs of tensile test workpieces. The micrographs revealed that multi-cracks were formed in the coatings. This was particularly true for Diamalloy 2002 coating, which contained 12% WC. In this case, the crack size was larger than those observed for Diamalloy 4010 coatings. The close examination of micrographs revealed that some section of the coating was peeled off while some other section adheres to the workpieces surface. This showed that cracks could not propagate to the coating and base material interface, so that coating did not conform the plastic deformation in the base material. This was more pronounced for two-layered coating. In this case, shear deformation at the interface of two coating layers was responsible for peeling of the coating. In the case of small cracks, the sliding and splitting deformation took place in the coating under the tensile load. The close examination of fracture surfaces showed that fracture was brittle and takes place through the splats boundary. This may be explained the oxide layer formed around some of the splats; in which case, splats rebounded through their oxide interfaces. The stringers, which were the oxide particles, acted as stress centers promoting the stress concentration in the coating. Consequently, during the tensile loading, these centers contributed significantly to the crack initiation and propagation in the coating. Moreover, at coating-base material interface adhesion failure was also

observed, which occurred locally due to the presence of interface impurities in this region.

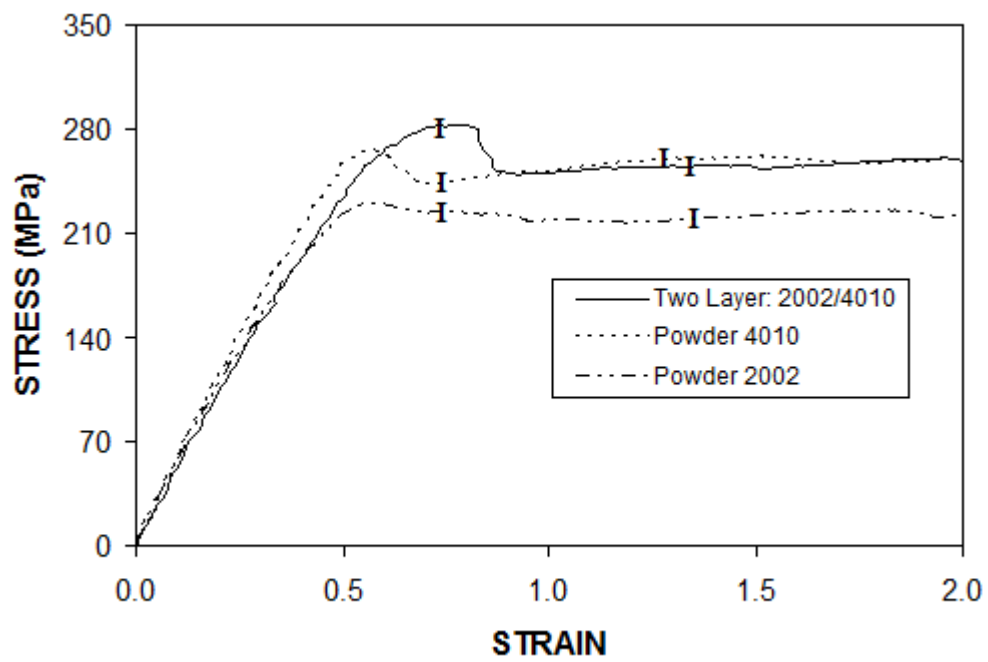
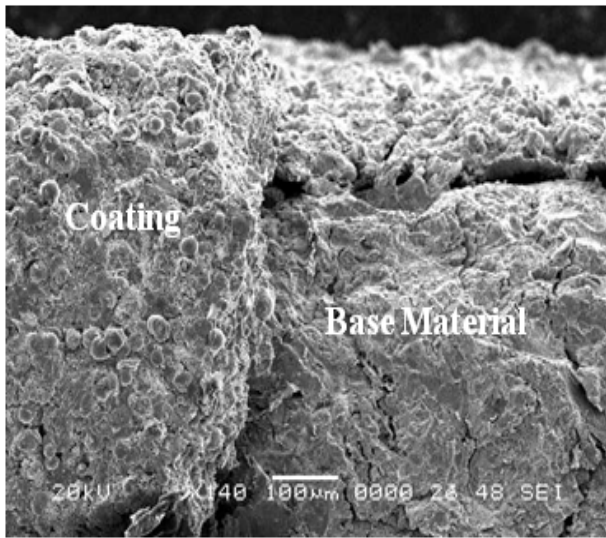
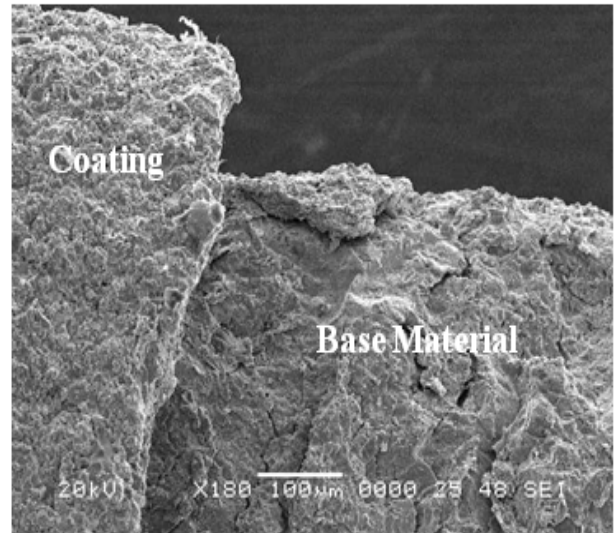


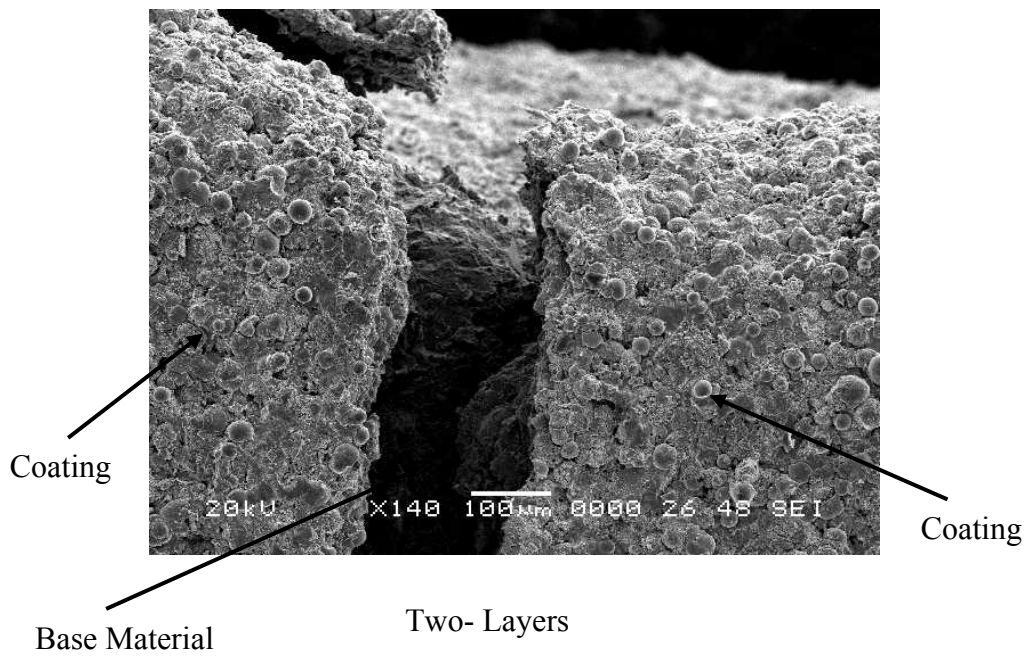
Figure 4.9 Stress-strain curve resulted from tensile tests
(Each curve result of three repeated tests)



Diamalloy 2002



Diamalloy 4010



Two- Layers

Figure 4.10 SEM micrographs of coating surfaces after tensile tests

Figure 4.11 shows load-displacement curve obtained from the three-point bending tests. It should be noted that three point bending was carried out at constant stress rate. The elastic-plastic behavior of the coatings, due to Diamalloy 2002 and Diamalloy 4010 as well as two layered structure, were different. The flexural displacement increased at low load levels for coating produced from Diamalloy 4010 powder while it was low for Diamalloy 2002 coating. This was attributed to the presence of WC content in the coatings, which made the coating stiffer and harder. The sudden drop in flexural displacement revealed the failure of the coating during the bending tests. This occurred after the long flexural displacement for Diamalloy 2002 coating and two-layered structure. Table 4.1 gives the elastic modulus determined from the three-point bending tests. It was evident that Diamalloy 2002 had the highest elastic modulus because of the presence of 12% WC in the coating.

Figure 4.12 shows SEM micrograph of fractured surface after three-point bending tests. Since the coating was applied at the top and bottom surface of the workpieces, coating failure was due to compression and tensile-shear. The extended crack formation at the bottom surface, where tensile-shear failure took place, was evident. However, in some region, the delimitation of coating occurred because of excessive shear stress developed in the coating during the bending test. In addition, the

presences of oxide particles contributed to the shear failure, particularly in the surface region of the coating. The tensile–shearing force enhanced the internal stresses while creating local stress concentrations in the coating. This was more pronounced at defect sites such as oxide particles in the coating. Consequently, stress concentrations at defect sites became higher than that of the mean internal stress. As bending progresses, a critical stress levels was reached at the defect sites. This triggered the large crack formation. However, the presence of defect sites at coating–base material interface resulted in the total failure of the coating, i.e. coating peeledoff from the base material surface. In the surface region, the crack propagation was limited with this region; in which case, small cracks were formed during the bending. However, if the energy dissipated during micro cracks formation, the crack propagation ceased and the microcracks were formed in the surface region. In addition the compressive stress developed at the top surface of the workpiece resulted in partial peeling of the coating in the surface region.

Table 4.2 Elastic modulus determined from three-point bending tests.

Diamalloy 4010 (GPa)	Diamalloy 2002 (GPa)
611	741

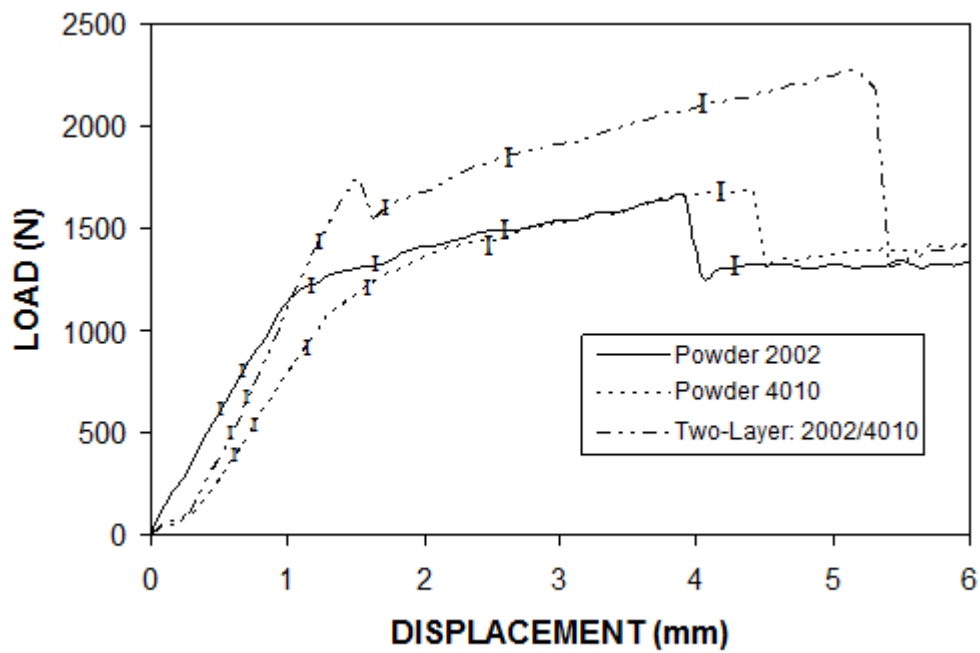
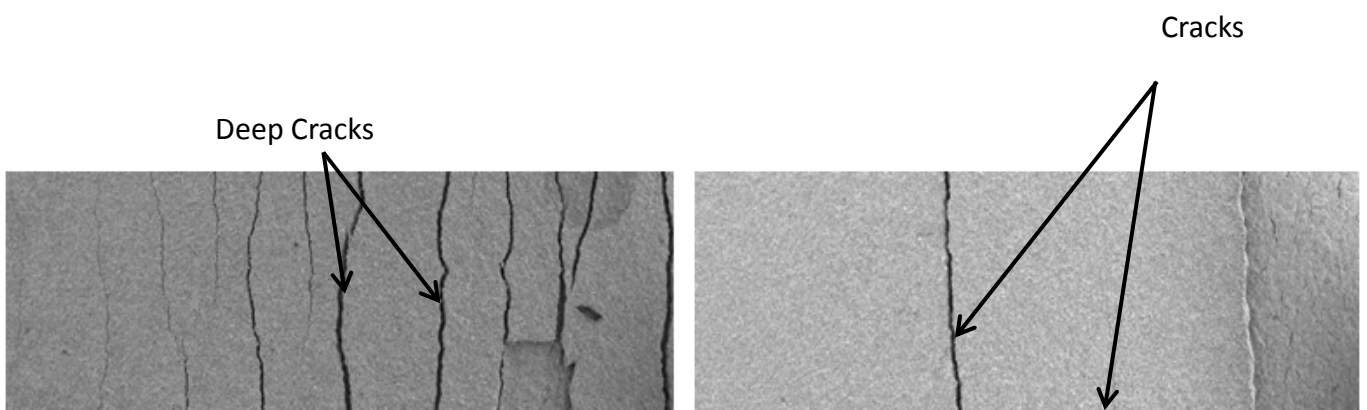
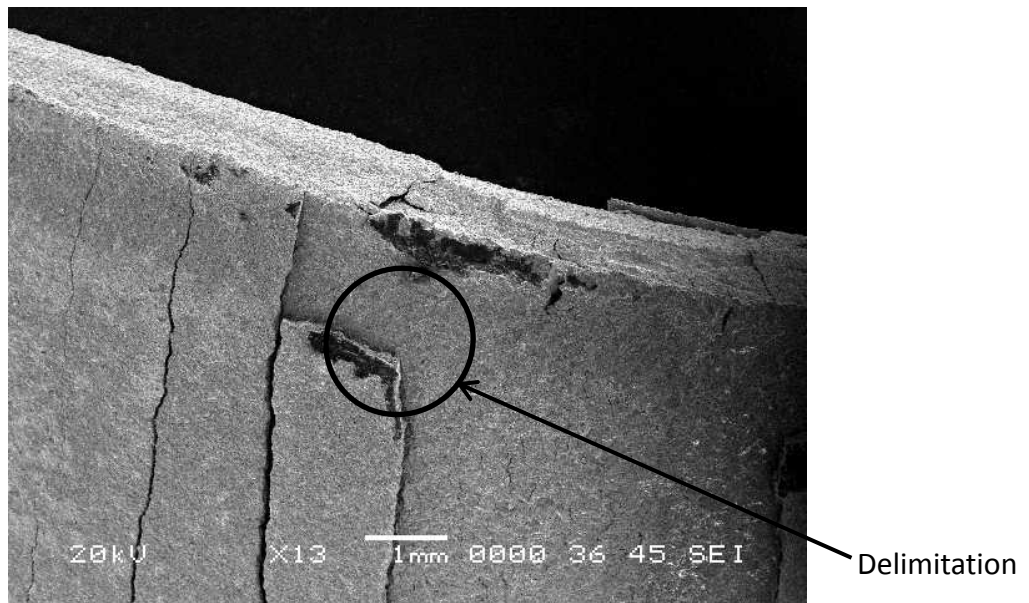
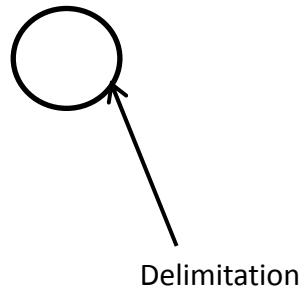


Figure 4.11 Load-displacement characteristics obtained from three-point bending tests.





Two- Layers

Figure 4.12 SEM micrographs of coating surfaces after three-point bending tests.

Chapter 5- Conclusions and Recommendations for Future Works

5.1 Conclusion

Study of HVOF coating of Diamalloy 2002 and 4010 powders onto the alloy steel surface was carried out. Two layered coatings, consisting of Diamalloy 4010 bottom layer and Diamalloy 2002 top layer, was realized. The microstructure of the resulting coating was examined using optical microscope, SEM and EDS. The indentation tests were carried out for the hardness and surface elastic modulus measurements. It was found that coatings produced from the Diamalloy 2002 and Diamalloy 4010 gave similar surface textures, provided that some scattered protruded splats were observed at the surface for Diamalloy 2002 coating. This could be related to the presence of contained WC, which had a high melting temperature. Coatings produced from both powders formed lamellar structures with the porosity of the order of 3%. No large cavities or irregularities were observed at the coating-base material interface, except Diamalloy 2002 coating. In this case, a locally extended line of discontinuous gap was observed. Oxidation of the some splat surface appeared as black inclusions in the coatings; however, the oxide layer did

not cover all the surface of the splats. The microhardness measurement revealed that the coating formed by using Diamalloy 2002 had higher hardness than that corresponding to Diamalloy 4010. This was attributed to the presence of WC in the splats. The elastic modulus determined from the indentation tests showed that the elastic modulus of the coating formed from Diamalloy 2002 was higher than that of Diamalloy 4010.

The mechanical properties of the coating were assessed through tensile and three-point bending tests. It was found that coating produced was free from the loose splats at the surface and free from large cracks and voids across the cross-section. The porosity for Diamalloy 2002 coating was higher than that of Diamalloy 4010 due to the presence of solid phase WC in the coatings. The presence of oxide splats was evident in the surface region of the coatings. The tensile behavior of the coating revealed that tensile load did not produce excessive number of cracks affecting the tensile behavior of the workpieces. However, the irregularities observed in the elastic limit of the curves indicated the formation of cracks in the coatings, which was particularly true for two layered coating. The shear stress developed at interface of the two-layered coating was responsible for the crack initiation in the coating. The deep cracks were also formed in the coatings after the tensile tests. This was attributed the local stress centers, which increased the stress intensity

under the tensile load. Moreover, once the crack was initiated, it propagated around the splat boundary, which was more pronounced for the oxidized splats in the surface region of the coating. Three-point bending tests revealed that tensile-shear failure in the coating occurred. In this case, the multiple cracks were developed for Diamalloy 4010 coating while deep and wide spaced cracks were formed for Diamalloy 2002 coating. The presence of defect sites at the coating-base material caused stress concentration in this region, which in turn resulted in the peeling-off the coating from the base material surface. In the surface region, small cracks were developed, which was attributed to oxidized splats and stress relieving through small side cracking in the surface region of the coating. The elastic modulus increased for Diamalloy 2002 coating due to the presence of 12% WC in the coating.

5.2 Recommendations for Future Works

The present study work dealt with the examination of some of the mechanical properties (tensile and three-point bending) of single and two layer coatings on alloy steel work pieces in relation to rotating equipment and oil industry application. This could be extended to include the following:

- Fatigue properties of two layer coatings.
- Corrosion resistance of two layer coatings.
- Wear behavior and erosion resistance of two layer coatings
- Influence of heat treatment at elevated temperature on mechanical and metallurgical characteristics of coatings. The heat treatment always reduced the residual stress of the coating which enhanced the tribological properties of the coating. The heat treatment conditions could be also selected to resemble the gas turbine hot gas path components such as liner, transition piece and turbine inlet nozzles.
- Influence of surface welding using a laser beam on the mechanical and metallurgical characteristic of two layer coatings. Laser melting provides formation of continuous hard film thus corrosion and wear resistance of coating could be improved.

Author Publications

- 1- Y.A. Al-Shehri, M.S.J. Hashmi, B.S. Yilbas, HVOF coating of Diamalloy 2002 and Diamalloy 4010 on steel sheets: microstructure examination, conference on Advances in Materials and Processing Technology, AMPT09, Kuala Lumpur, Malaysia November 26-29, 2009.
- 2- Y.A. Al-Shehri, M.S.J. Hashmi, B.S. Yilbas, HVOF coating of Diamalloy 2002 and Diamalloy 4010 onto steel: Tensile and bending response of coating , conference on Advances in Materials and Processing Technology, AMPT10, Paris, France October 24-27, 2010.

Reference

- [1] J. Stokes, “*Theory and Application of SulzerMetco High Velocity Oxy-Fuel (HVOF) Thermal Spray Process*”, © Dublin City University (2008), ISBN 1-87232-753-2, ISSN 1649-8232.
- [2] J.R. Davis & Associates, *ASM Hand Book of Thermal Spray Technology*, (2004), ISBN: 0-87170-795-0.
- [3] P. Gao, G. Yang, C. Li, C. Li, Preparation of Multimodal Structured WC-12Co Deposits by Cold Spraying, International Thermal Spray Conference & Exposition, (2008), pp. 1202-1207.
- [4] M.F. Morks, Yang Gao, N.F. Fahim and F.U. Yingqing, Microstructure and hardness properties of cermet coating sprayed by low power plasma, *Materials letters*, 60, 2006, pp. 1049-1053.
- [5] SulzerMetco, [online], www.sulzermetco.com (Access date 2010).
- [6] J. Berget, 1998. Influence of Powder and Spray Parameters on Erosion and Corrosion Properties of HVOF Sprayed WC-Co-Cr coatings. Ph.D. Thesis, Norwegian University of Science and Technology, Engineering Material Science, (1998), Norway.
- [7] M. Kaur, H. Singh, Fatehgarh Sahib/IND, and S. Prakash, Roorkee/IND, Hot corrosion and high temperature oxidation performance of WC-Co coatings by detonation-gun spray on a boiler steel, ITSC-2008 conference proceeding, 2008, pp. 423-428.
- [8] Y. Itoh, M. Saitoh and M. Tamura, Characteristics of MCrAlY Coating Sprayed By High Velocity Oxygen –Fuel Spraying System, *Journal of Engineering for Gas Turbines and Power*, 122, 2000, pp. 43-49.

- [9] Gordon England, [online], www.gordonengland.co.uk, (Access date 2008).
- [10] J. Koutsky, High velocity oxy-fuel spraying, *Journal of Materials Processing Technology*, 157-158, 2004, pp. 557-560.
- [11] R.S. Lima and B.R. Marple, Optimized HVOF Titania Coatings, *Journal of Thermal Spray Technology*, 12(3), September 2003, pp. 360-369.
- [12] L. Fedrizzi, S. Rossi, R. Cristel, P.L. Bonora, Corrosion and wear behavior of HVOF cermet coatings Used to replace hard chromium, *Electrochimica Acta*, 49, 2004, pp. 2803-2814.
- [13] Y. Wang, C. Li, A. Ohmori, Examination of factors influencing the bond strength of high Velocity oxy-fuel sprayed coatings, *Surface & Coating Technology*, 200, 2006, pp. 2923-2928.
- [14] A. Boudi, M.S.J. Hashmi, and B.S. Yilbas, ESEM Evaluation of Inconel-625 thermal spray coating (HVOF) onto stainless steel and carbon steel post brine exposure after tensile test, *Journal of Materials Processing Technology*, 173, 2006, pp. 44-52.
- [15] J. Tan, Looney, M.S.J. Hashmi, Component Repair using HVOF thermal spraying, *Journal of Materials Processing Technology*, 92-93, 1999, pp. 203-208.
- [16] Y. Qiao, T. Fischer and A. Dent, The effects of fuel chemistry and feed stock powder structure on the mechanical and tribological properties of HVOF thermal-sprayed WC-Co coatings with very fine structures, *Surface and Coatings Technology*, **172**, 2003, pp. 24-41.
- [17] Advance Surface Technology, [online], www.surfacetchno.com, (Access date 2008).
- [18] D. Stewart, P. Shipway, D.G. McCartney, Influence of heat treatment on the abrasive wear behavior of HVOF sprayed WC-Co coatings, *Surface and Coatings Technology*, **105**, 1998, pp. 13-24.

- [19] K. Padilla, A. Velasquez, J. A. Berrios, E.S. Cabrera, Fatigue Behavior of 4140 Steel coated with a NiMoAl deposit Applied by HVOF Thermal Spray, *Surface & Coating Technology*, **150**, 2002, pp.151-162.
- [20] J.M. Guliemany, J. Fernandez, J. Delgado, A.V. Benedetti, F. Climent, Effects of thickness coating on the electrochemical behavior of thermal spray Cr₃C₂-NiCr coatings, *Surface & Coating Technology*, **153**, 2002, pp. 107-113.
- [21] V. Stoica, R. Ahmed M.Golshan and S. Tobe, Silding Wear Evaluation of Hot Isostatically Pressed Thermal Spray Cermet Coatings, *Journal of Thermal Spray Technology*, **13(1)**, March 2004, pp. 93-107
- [22] C.N. Machio, G. Akdogan, M.J. Witcomb, S. Luyckx, Performance of WC-VC-Co thermal spray coating in Abrasion and slurry erosion tests, *Wear*, **258**, 2005, pp. 434-442.
- [23] B. Wielage, A. Wank, H. Pokhmurska, T. grund, C. Rupprecht, G. Reisel and E. Friesen, Development and Trends in HVOF Spraying Technology, *Surface & Coating Technology*, **201**, 2006, pp. 2032-2037.
- [24] H.Y. Al-Fadhli, J. Stokes, M.S.J. Hashmi and B.S. Yilbas, The erosion-corrosion behavior of high velocity oxy-gen fuel (HVOF) thermally sprayed inconel-625 coatings on different metallic surfaces, *Surface & Coating Technology*, **200**, 2006, pp. 5782-578.
- [25] Y. Wang and S. Lim. Tribological behavior of nanostructured WC particles/polymer coatings, *wear*, **262**, 2007, pp. 1097-1101.
- [26] G.Reisel, B. Wielage, S. Steinhauser, I. Morgenthal and R. Scholl, High temperature oxidation behavior of HVOF-Sprayed unreinforced and reinforced molybdenum disilicida powders, *Surface and Coatings Technology*, **146-147**, 2001, pp. 19-26.
- [27] T.C. Totemeier, R.N. Wright and W.D. Swank, Microstructure and stresses in HVOF Sprayed Iron Aluminide Coatings, *Journal of Thermal Spray Technology*, **11(3)**, September 2002, pp.400-408.
- [28] W.J. Trompetter, A. Markwitz and M. Hyland, Role of oxides in high velocity thermal spray coatings, *Nuclear Instruments and Methods in Physics Research B*, **190**, 2002, pp. 518-523.

- [29] B. Hwang, S. Lee, and J. Ahn, Correlation of microstructure and wear resistance of molybdenum blend coating fabricated by atmospheric plasma spraying, *Material Science and Engineering*, **A366**, 2004, pp.152-163.
- [30] W. Hu, M. Li and M. Fukumoto, Preparation and properties of HVOF NiAl nanostructured coatings, *Material Science and Engineering A*, **478**, 2008, pp. 1-8.
- [31] P. Gao, C. Li , G. Yang, Y. Li, C. Li, Influence of substrate hardness on deposition behavior of single porous WC-12Co particle in cold spraying, *Surface and Coatings Technology*; Vol. 203, Issues 3-4, 25 November 2008, pp. 384-390.
- [32] G. Goulaouen,, “Influence of Spray Parameters on Stainless Steel Coating Properties”,Proceeding of the 15th ITS in Nice, France, 1998, pp. 537-545.
- [33] W.C. Lih, S.H. Yang, C.Y. Su, S.C. Huang, I.C. Hsu and M.S. Leu, Effects of process parameters on molten particle speed and surface temperature and the properties of HVOF CrC/NiCrcoatings,*Surface and Coatings Technology*,**133-134**,2000,pp.54-60.
- [34] S. Kuroda, Y. Tashiro, H. Yumoto, S. Taira, H. Fukanuma and S. Tobe. Peening Action and Residual Stresses in High Velocity Oxygen Fuel Thermal Spraying of 316L Stainless Steel, *Journal of Thermal Spray Technology*, **10(2)**, June 2001, pp. 367-374.
- [35]T.C. Totemeier, R.N. Wright and W.D. Swank, Residual Stresses in High Velocity Oxy-Fuel Metallic Coatings, *Metallurgical and material Transactions*,**Vol. 35 A**, June 2004, pp.1807-1814.
- [36] T.C. Totemeier, R.N. Wright and W.D. Swank, Mechanical and Physical Properties of High-VelocityOxy-Fuel-Sprayed Iron Aluminide Coatings, *Metallurgical and material Transactions A*, **34A**, October 2003, pp. 2223-223.
- [37] L. Zhoa, M. Maurer, F. Fischer, R. Dicks and E. Lugscheider, Influence of spray parameters on the particle in-flight properties and the properties of HVOF coating of WC-CoCr, *Wear*, **257**, 2004, pp. 41-46.

- [38] M. Hasan, J. Stokes, L. Looney, M.S.J. Hashmi, Effect of spray parameters on residual stress build-up of HVOF sprayed aluminum/tool-steel functionally graded coatings, *Surface & Coating Technology*, **202**, 2008, pp.4006-4010.
- [39] Y. Shimiz, K. Sugiura, “ An Attempt to Improve the Deposition Efficiency of (Al₃O₃) Coating by HVOF Spraying”, Proceeding of the 1st International Thermal Spray Conference on Surface Engineering Via Applied Research, Pub ASM International, Material Park, OH, USA, 2000, pp. 181-186.
- [40] M.P. Nascimento, R.C. Souza ,W.L. Pigatin, H.J.C. Voorwald, Effects of surface treatments on the fatigue strength of AISI 4340 aeronautical steel ,*International Journal of Fatigue*, Volume 23, Issue 7, August 2001, pp. 607-618.
- [41] R. Ahmed and M. Hadfield, Mechanisms of Fatigue failure in thermal Spray coatings, *Journal of Thermal Spray Technology*, **11(3)**, September 2002, pp.333-349.
- [42] J. Wang, K. Li, D. Shu, X. He, B. Sun, Q. Guo, M. Nishio, H. Ogawa, Effects of Structure and Processing Technique on the Properties of Thermal Spray WC-Co and NiCrAl/WC-Co coatings, *Material Science and Engineering*, **A371**, 2004, pp.187-192.
- [43] S.Sampath, X.Y. Jiang, J. Matejicek, L. Prchlik, A. Kulkarni and A. Vaidya, Role of thermal spray processing method on the microstructure, residual stress and properties of coatings; an integrated study for Ni-5 wt.%Al bond coats, *Material Science and Engineering* , **A364**, 2004, pp. 216-231.
- [44] B.S. Yilbas, A.F.M. Arif and M. Gondal, HVOF coating and laser treatment: three-point bending tests, *Journal of Material Technology*, **164-165**, 2005, pp.954-957.
- [45] P. Chivavibul, M. Watanabe; S. Kuroda; J. Kawakita; M. Komatsu; Tsukuba/J, K. Sato, J. Kitamura, Development of WC-Co coatings deposited by warm spray process, International Thermal Spray Conference & Exposition 2008: Thermal Spray Crossing Borders (DVS-ASM);2008, pp.54-58.

- [46] West Yorkshire Steel Company, [online], www.westyorkssteel.com, (Access date 2008).
- [47] ASTM E8, “Standard Method of Tension Testing of Metallic Materials”, American Society for Testing and Material Standards, Philadelphia, (2004).
- [48] C. Coddet, G. Montavon, S. Ayrault-Costil, O. Freneaux, F. Rigolet, G. Brbezat, F. Folio, A. Diard and P. Wazen, Surface preparation and thermal Spray in a Single step: The Portal Process-Example of Application for an Aluminum-Base Substrate, *Journal of Thermal Spray Technology*, Vol.8(2), 1999, pp.235-242.
- [49] H. Li, K.A. Khor and P. Cheang, Young’s modulus and fracture toughness determination of high velocity oxy-fuel-sprayed bioceramic coatings, *Surface & Coating Technology*, **155**, 2002, pp.21-32.
- [50] ASTM D 790, “Standard Test Methods for Flexural Properties of Unreinforced and Reinforced Plastics and Electrical Insulating Materials”, American Society for Testing and Material Standards, Philadelphia, (2003).
- [51] P.G. Charalambides, J. Lund, A.G. Evans, R.M. McMeeking, Test specimen for determining the fracture resistance of bimaterial interfaces, *J. Applied Mechanics*, **56**, 1989, pp. 77-82.
- [52] N. Fawcett, Novel method for the measurement of Young's modulus for thick-film resistor material by flexural testing of coated beams, *Measurement Science and Technology*, **9**, 1998, pp. 2023-2026.
- [53] Instron, [online], www.instron.com, (Access date 2010).
- [54] Y. Qiao, T. E. Fischer, A. Dent, The effects of fuel chemistry and feedstock powder structure on the mechanical and tribological properties of HVOF thermal-sprayed WC-Co coatings with very fine structures, *Surface and Coatings Technology*, **172**, 2003, pp. 24-41.
- [55] K. Niihara, R. Morena, D.P.H. Hasselman, Indentation fracture toughness of brittle materials for palmqvist cracks, *Fracture Mechanics of Ceramics*, **5**, 1983, pp. 97-105.

[56] H. Li, K. A. Khor, and P. Cheang, Young's modulus and fracture toughness determination of high velocity oxy-fuel-sprayed bioceramic coatings, *Surface and coating Technology*, **155**, 2002, pp. 21-32.

[57] Struers, [online], www.struers.com, (Access date 2010).

[58] D. Al-Anazi, M.S.J. Hashmi and B.S. Yilbas, HVOF thermally sprayed CoNiCrAlY coatings on Ti-6Al-4V alloy: high cycle fatigue properties of coating, *Proc. Inst. Mech. Engrs., Part B, Journal of Engineering Manufacture*, **221**(2007) 647-654.

[59] D. Al-Anazi, M.S.J. Hashmi and B.S. Yilbas, HVOF coating of AMDRY 9954 onto Ti-6Al-4V alloy: fracture toughness measurement, *Proc. Inst. Mech. Engrs., Part B, Journal of Engineering Manufacture*, **221**,2007, pp.617-623.

[60] Z.Y. Taha-al, M.S.J.Hashmi, B.S. Yilbas, Laser treatment of HVOF coating: model study and characterization, *J. Mechanical Science and Technology*, **21**, 2007, pp. 1439-1444.